Zamorano University

Food Science and Technology Department

B.S. in Food Science and Technology

Special Graduation Project

“Fiber and Anthocyanin Mixtures for Improved Butyrate Production in Pediatric UC-Associated Fecal Microbiota”

Student

Sarah Eliana Quino Gutierrez

Advisors

Ligia Luna, M.Sc.

Lavanya Reddivari, Ph.D.

Edward Moncada, Ph.D.

Honduras, November 2025

Authorities

KEITH L. ANDREWS

President a.i.

ANA M. MAIER ACOSTA

Vice President and Academic Dean

ADELA ACOSTA MARCHETTI

Director of Food Science and Technology Department

JULIO NAVARRO

Secretary General

Table of Contents

List of Tables

List of Figures

List of Appendices

Abstract

A considerable amount of research has been conducted on the recognition of the efficacy of dietary fibers and anthocyanins in modulating microbiota. However, their combined interaction in the context of ulcerative colitis (UC) remains unclear. The objective of this study was to determine the effects of fiber mixtures alone and in combination with anthocyanins on the efficiencies of colonic fermentation associated with short-chain fatty acid (SCFA) production. Including possible synergisms, with emphasis on butyrate, as an important metabolite in gut health and UC management. *In vitro* fermentations were performed with pooled stool samples from two pediatric UC donors, and the treatments were assessed at various time points (0, 12, 24, and 48 hours). To assess fermentation outcomes, pH, gas, SCFA, and butyrate production were measured. Further, the results were complemented by microbial profiling to confirm shifts in the microbiota. The results have indicated that the physicochemical properties of the fibers in fiber mixture B (FMB) favor the interaction between the fibers and anthocyanins, thereby improving the performance of fermentation. This resulted in a greater butyrate and more balanced SCFA profile production per mL of gas produced than what was observed with the single fiber mixture. These results confirm that the interactions between fiber and anthocyanin can enhance fermentation results. The following steps involve verifying these results using *in vivo* systems and clinical studies. This will help continue to assess the effects of anthocyanins and fiber mixtures on inflammation and symptoms in UC.

Keywords: fermentation; gut microbiota; polyphenol; short-chain fatty acids (SCFA); synergy

Resumen

Existen investigaciones sobre la eficacia de las fibras dietéticas y las antocianinas en la modulación de la microbiota. Sin embargo, aun no se ha investigado a profundidad sus efectos en colitis ulcerativa (CU). El objetivo de este estudio fue determinar los efectos de las mezclas de fibras diseñadas solas y en combinación con antocianinas en mejorar los productos y eficiencia de la fermentación colónica. Esto con énfasis en la producción de ácidos grasos de cadena corta (AGCC), especialmente butirato, incluyendo posible sinergia entre ambos compuestos. Se realizaron fermentaciones *in vitro* con muestras mixtas de heces de donantes pediátricos de CU. Los tratamientos fueron evaluados a las 12, 24 y 48 horas. Se midió la producción de pH, gas, SCFA, y butirato durante la fermentación. Se complementaron los resultados de este estudio con un perfil microbiano adicional para confirmar los cambios en la microbiota. Los resultados indicaron que la interacción entre las fibras de FMB y antocianinas mejoró el rendimiento de fermentación. Esto mejoró la producción de butirato y SCFA por mL de gas, indicando sinergia entre ambos componentes. Por otra parte, los tratamientos con mezclas de fibras A (FMA) no demostraron este efecto. Esto indica que la sinergia es dependiente de las características fisicoquímicas de la mezcla de fibras. Los siguientes pasos implican verificar estos resultados con sistemas *in vivo* y estudios clínicos, que impliquen la evaluación de los efectos de las antocianinas junto con las fibras sobre la inflamación en UC.

Palabras clave: ácidos grasos de cadena corta (AGCC); fermentación; microbiota intestinal; polifenoles; sinergia

Introduction

While extensive research has been conducted on inflammatory bowel diseases (IBD), ulcerative colitis (UC), a subform of IBD, still represents a significant clinical challenge (Fukuda et al., 2019). Patients with UC report continuous inflammation of the colonic mucosa, leading to symptoms such as diarrhea, abdominal pain, rectal bleeding, fatigue, and unintended weight loss (Kobayashi et al., 2020). UC was traditionally considered a condition of adulthood. However, recent data indicate an alarming increase in its prevalence among children and adolescents (Mutaz, 2024). In the United States alone, the incidence of this disease has risen by approximately 29% compared with estimates from 2009, with around 36,000 pediatric patients currently affected (Kappelman et al., 2025).

This chronic disease has an unclear pathogenesis, which makes it difficult to develop treatments for the long-term. This challenge is even more concerning in pediatric patients, as the disease often becomes more aggressive as it progresses (Yarur et al., 2011). Here, conventional pharmacological treatments, while effective in the short term, may contribute to further adverse effects over time (Cross, 2017). Given these limitations, dietary approaches emerge as more sustainable alternatives, including specific compounds that may work together to help manage UC symptoms (H. Li et al., 2020).

Although, the origin of UC pathogenesis is unclear, it is believed to be triggered by potential risk factors such as, genetic predisposition, lowered diversity in the microbiota and environmental factors such as western dietary patterns high in fat and sugar, and especially low in fiber (Li et al., 2020). In healthy individuals, fiber consumption is widely known for nourishing gut microbes, thus supporting immune and metabolic health, yet a lower intake of fiber is associated with a greater risk of developing UC (Facchin et al., 2024; Milajerdi et al., 2021). Interestingly, once UC is present, patients report low fiber intolerance due to gastrointestinal distress caused by fiber metabolism (Armstrong et al., 2023). This fiber intolerance is closely linked with alterations in gut microbial composition and a reduction in diversity, also known as dysbiosis (Ananthakrishnan, 2015). Dysbiosis is a widely known

hallmark of UC. Its presence is associated with worsening of the epithelial barrier breakdown, immune dysregulation, and chronic inflammation (Di Vincenzo et al., 2024). Likewise, it is characterized by disrupting the balance of pro- and anti-inflammatory bacterial species, reducing the production of beneficial metabolites such as short-chain fatty acids (M. Zhang et al., 2017).

Although pharmacological interventions such as corticosteroids, immunomodulators, and biologics are standard treatments for UC, they often carry substantial risks when used in the long term (Cross, 2017). Corticosteroids, for instance, are associated with serious side effects, including osteoporosis, hypertension, and neuropsychiatric disturbances (Bruscoli et al., 2021). Furthermore, biologic therapies, while effective for some patients, can lead to loss of response over time and increased susceptibility to infections (Steinsbø et al., 2022).

Beyond conventional treatments, the composition and function of the gut microbiota are key to maintaining intestinal homeostasis (Lee et al., 2022). Bacteria that produce butyrate are central to this balance and are often categorized into primary, secondary, and tertiary fermenters that cross-feed on metabolic by-products (Lozupone et al., 2012). In UC patients, this microbial interaction is disrupted, with a significant reduction in butyrate producers, composed mainly of tertiary fermenters, such as *Faecalibacterium prausnitzii*, *Roseburia spp*., and members of the *Clostridium cluster XIVa* (Thaisa M. Cantu-Jungles et al., 2021; Machiels et al., 2014). This reality underscores the necessity for sustainable and dietary-oriented strategies that promote the production of beneficial metabolites during colonic fermentation, helping in the management of UC in the long term in pediatric patients.

Dietary fibers, defined as non-digestible carbohydrates, emerge as potential alternatives that promote gut bacterial diversity by acting as prebiotics and reducing inflammation (Kabisch et al., 2025; Lachmansingh et al., 2023). They pass through digestion and reach the colon, where they are fermented by gut microbes into SCFAs like acetate, propionate, and butyrate (Makki et al., 2018). This fermentation process modulates immune function, promotes regulatory T cell differentiation, and strengthens the gut barrier (Zhang et al., 2023). Butyrate, particularly, serves multiple critical roles as

it is the preferred energy source for colonocytes, which enhances epithelial barrier integrity and exerts anti-inflammatory effects (Park et al., 2024). These properties are achieved through the modulation of nuclear factor kappa-light-chain-enhancer of activated B cells (NF-κB), inhibition of histone deacetylases (HDACs), and activation of G-protein-coupled receptors (GPCRs), such as GPR43 and GPR109A (Parada Venegas et al., 2019).

Dietary fiber mixtures are combinations of structurally diverse fibers. A study by T. M. Cantu-Jungles et al. (2025) demonstrated that the combination of structurally diverse fibers act synergistically to promote microbial diversity. Thereby increasing benefic and important taxa. Moreover, they have shown greater efficacy in consistently enriching butyrate-producing bacteria across individuals than single-fiber interventions (Cantu-Jungles y Hamaker, 2023).

Despite their benefits, fibers have traditionally been linked to gastrointestinal discomfort under UC conditions. This is due to their association with bloating and gas production. (Aliu et al., 2024). However, Moncada et al. (2024) revealed that selecting fibers based on favorable physicochemical properties, such as fermentability, complexity, and solubility, can ameliorate these effects by promoting beneficial microbial activity and enhancing short-chain fatty acid production. Thus, improving fiber tolerance. Regarding relevant physicochemical characteristics of fibers, fermentation rate influences the temporal profile of SCFA release, while moderate rates are preferable for sustained butyrate availability (Tuncil et al., 2018). Solubility affects the accessibility of fiber to microbial enzymes, while viscosity can modulate gut transit time and mucosal interaction (Nagano et al., 2025). Complexity, defined by the degree of branching and glycosidic linkages, determines selective utilization by beneficial bacteria and can help suppress opportunistic pathogens (Hamaker y Tuncil, 2014).

Alongside fiber, anthocyanins, which are bioactive compounds, have emerged as promising dietary components for UC management. They are known for their antioxidant, anti-inflammatory, and anti-carcinogenic properties (Khoo et al., 2017). However, anthocyanins are unstable molecules.

Their structure degrades easily with changes in pH, light, heat, oxygen or enzyme action (Srinivasan y Rana, 2025). It has been demonstrated that combining anthocyanins into a food matrix helps protect them and increase their stability (Tang et al., 2023). For instance, Maiuolo et al. (2024) demonstrated that complexation of dietary fibers plus polyphenols boosts the production of SCFAs during fermentation, particularly butyrate concentrations. Furthermore, in an *in vivo* UC context, anthocyanin and pectin complexes have demonstrated great potential as UC treatments. This, by increasing anthocyanin stability and sustaining colonic delivery, where they help regulate inflammation (Eckrote y Reddivari, 2025). Finally, various studies have proven that anthocyanins promote the growth and metabolic activity of butyrate-producing bacteria, thereby supporting SCFA production (Ozdal et al., 2016; Verediano et al., 2021).

Therefore, this study aims to determine whether dietary fibers and anthocyanin combinations can enhance butyrate concentration and reduce gas production under pediatric UC dysbiosis. Additionally, it aims to determine whether the physicochemical characteristics of fibers affect their interaction with anthocyanins, thereby enhancing fermentative capacity.

Material and Methods

Study Location

This study was conducted in the Functional Foods for Gut Health Laboratory within the Department of Food Science at Purdue University (West Lafayette, Indiana, USA), from January to April 2025.

Project Planning

The methodology employed in this study was structured into three main phases: Phase 1 involved laboratory-simulated upper gastrointestinal (GI) digestion, Phase 2 involved *in vitro* anaerobic fermentation, and finally, Phase 3 involved data collection. Additionally, the physicochemical characteristics. This organization provided a more comprehensive understanding of how fiber and anthocyanins influence gut microbial metabolism in a laboratory-simulated digestion process.

Selection of Fiber Composition and Rationale

First, Table 1 shows the physicochemical characteristics of each fiber mixture, based on the reviewed literature of their fiber components. This will enable a better understanding of how specific physicochemical characteristics may influence the outcomes of each treatment through each fiber formulation and fiber-anthocyanin interactions.

Table 1

Overall physicochemical characteristics of fiber mixtures

Physicochemical characteristics of fiber mixtures				
Fiber Mix	Fermentability Rate	Complexity	Solubility	Viscosity
FMA	Slower fermentable portion	Lower complex portion	Lower soluble portion	Lower overall viscosity
FMB	Faster fermentable portion	Higher complex portion	Higher soluble portion	Higher overall viscosity

Note. Table 1 summarizes the physicochemical traits of the two fiber mixtures, including flexibility, complexity, solubility, and viscosity. These values were compiled from reviewed literature and organized to highlight whether each characteristic is present in higher or lower amounts. This overview helps illustrate how the fibers differ in structural behavior and potential interactions during fermentation.

This table shows the two fiber mixtures and their overall physicochemical characteristics. This information was obtained from a review of the literature on the properties of each of their fiber components. The relevant physicochemical properties investigated were fermentability rate, complexity, solubility, and viscosity. In this sense, Fiber Mixture A (FMA) was classified to have a slower fermentable fraction, lower solubility, lower complexity, and lower viscosity. In contrast, Fiber Mixture B (FMB) was classified as having a faster fermentable fraction, higher structural complexity, higher solubility, and higher viscosity.

Simulated Upper Gastrointestinal (GI) Digestion

The upper GI digestion phase simulates the physiological conditions of the human digestive system, involving the oral, gastric, and small intestine stages. This phase follows the simulated digestion process using the standardized INFOGEST 2.0 protocol (Brodkorb et al., 2019), with minor adjustments to target the digestion of fiber. This protocol incorporates specific enzyme concentrations, pH adjustments, and specific time periods to mimic *in vivo* digestion.

The purpose of this phase is to break down dietary components, such as simple carbohydrates and sugars, releasing undigestible compounds that will later be available for microbial metabolism in the colon. This replicates the conditions of the GI tract and diffuses broken components through the permeable bag, ensuring that only fiber substrates enter the fermentation stage, thereby resembling real physiological conditions.

Sample Preparation for Upper GI Digestion

A total of 9 commercial fibers were utilized in this study. Each fiber was bought commercially from an online supplier or donated by collaborating laboratories. Each fiber was prepared by weighing

5 g of each sample in two 50 mL labeled centrifuge tubes, giving a total of 10 grams initially per fiber. The total number of fibers was subjected to digestion.

The Anthocyanin Source Powder (AP) used in this study was not subjected to the digestion process and was directly incorporated in the *in vitro* fermentation step. This allowed us to directly assess potential anthocyanin interaction with fiber matrices. To prepare the AP, the original food matrix was first frozen and then freeze-dried. The resulting dry product was ground into a fine powder and kept on controlled temperature conditions (-20 °C) to prevent anthocyanin degradation.

To accurately model digestion, the steps of the protocol INFOGEST 2.0 procedure were followed. The digestion process is divided into three sequential phases: oral, gastric, and intestinal, each designed to simulate the physiological conditions of human digestion.

Oral Phase

The oral phase is the first step of digestion. Here, food is mixed with salivary solution to breakdown starch. In the simulated digestion, this phase includes preparing the enzyme solution so that it reaches a final activity of 75 U/mL when added to the sample.

Amylase Calculation

To simulate the enzymatic activity present during the oral phase of digestion, salivary amylase was incorporated into the reaction system at a final activity of 75 U/mL, according to INFOGEST 2.0 protocol. This preparation involved calculating the volume and concentration of a stock salivary amylase solution that would achieve this final activity when added to each sample. The commercially available salivary amylase used had a specific activity of 1000 U/mg.

Given that the oral phase volume for each sample was 10 mL, and that 0.5 mL of enzyme solution had to be added to each sample, the required activity of the enzyme stock solution was calculated using the dilution principle.

$$Final\ activity = \frac{Stock\ activity * Volume\ Added}{Total\ reaction\ volume} \quad [1]$$

For the required stock activity, we replace all the data, resulting in the required activity of 1500 U/mL.

$$75\ U/mL = \frac{X\ U/mL * 0.5\ mL}{10\ mL} \quad [2]$$

The stock solution had to contain 1500 U/mL of activity. Given the specific activity of 1000 U/mg, the corresponding mass concentration needed was 1.5 mg/mL.

$$75\ U/mL = \frac{1500\ U/mL}{1000\ U/mL} \quad [3]$$

To prepare this solution, 1 mg of enzyme powder was dissolved in 0.667 mL of deionized water, giving the desired concentration of 1.5 mg/mL, equivalent to 1500 U/mL. For the preparation of 8 samples, a total of 4 mL of enzyme stock solution was required (0.5 mL × 8). To account for pipetting loss and ensure consistency, 9 mg of enzyme was weighed and dissolved in 6 mL of water, maintaining the same concentration of 1.5 mg/mL.

The resulting enzyme stock solution was then added to the oral phase master mix at a volume of 0.5 mL per sample, giving a final enzyme activity of 75 U/mL in the 10 mL oral volume.

Oral digestion Process

Before starting the oral phase, SSF was prepared and kept in the incubator at 37 °C at least 15 minutes before the procedure started. The composition of the simulated salivary fluid can be found in Table 1, concluding this section, where the electrolyte solutions and stock concentrations used in this step are listed. Each fiber sample (5 g) was mixed 1:1 (wt/wt) with simulated salivary fluid (SSF). The calculated amount of salivary amylase was added to reach 75 U/mL. Calcium chloride dihydrate [$CaCl_2(H_2O)_2$] (0.15 mM final concentration) was incorporated. Additionally, pH was continuingly monitored to be at 7.0. Finally, incubation was conducted at 37 °C for 5 minutes with continuous agitation at 150 rpm.

Gastric Phase

The gastric phase is the second step of digestion. At this stage, the oral bolus enters an acidic environment where proteins begin to break down. The key enzyme here is pepsin, which was prepared to reach a final activity of 2000 U/mL in each sample. The bolus was mixed with simulated gastric fluid, calcium was added, and the pH was adjusted to 3.0 before incubation.

Pepsin Calculation

To replicate the enzymatic conditions of the gastric phase, pepsin was incorporated into the reaction at a final activity of 2000 U/mL, as specified by the standardized static *in vitro* digestion protocol. The commercial pepsin used had a measured specific activity of 3200 U/mg.

Each individual tube consisted of 20 mL total volume, composed of the oral phase (10 mL), simulated gastric fluid (8 mL of SGF 1.25×), calcium chloride (0.005 mL), pepsin solution (0.5 mL), acid/base (0.1 mL), and water (1.395 mL).

The final concentration of pepsin in the gastric phase was intended to be 2000 U/mL. Given the specific activity of pepsin (3200 U/mg), the amount of pepsin needed per sample was calculated based on the final activity desired, multiplied by the total gastric volume.

$$Final\ activity\ per\ sample = Final\ Activity * Total\ Gastric\ Volume$$

$$Final\ activity\ per\ sample = 2000\ U/mL * 20\ mL = 40{,}000\ U$$

Given the specific activity of pepsin (3200 U/mg), the corresponding quantity of enzyme needed per sample was 12.5 mg.

$$Enzyme\ Mass\ Per\ Sample = \frac{40{,}000\ U}{3200\ U/mg} = 12.5\ mg \quad [4]$$

To compensate for handling variability, 16 mg of pepsin was weighed per sample, slightly above the quantity required (12.5 mg), providing a safety margin. This amount was dissolved in 0.64 mL of water, resulting in a stock concentration of 25 mg/mL, equivalent to 80,000 U/mL.

According to the protocol, the volume required of the enzyme solution was 0.5 mL, then the actual activity per sample was 40,000U. When poured into the total gastric volume for each sample (20 mL), it resulted in the desired quantity of 2,000U.

Gastric digestion Process

The oral bolus was mixed 1:1 (vol/vol) with Simulated Gastric Fluid (SGF), incorporating calcium chloride dihydrate [$CaCl_2(H_2O)_2$]. The composition of the simulated gastric fluid is described in Table 1, where the electrolyte solutions and stock concentrations used in this phase are outlined. Further, the previously calculated amount of pepsin was added to a final concentration of 2,000 U/mL. pH was adjusted to 3.0 using 5 M HCl. Finally, samples were incubated at 37 °C for two hours with continuous mixing (150 rpm).

Intestinal Phase

The intestinal phase is the final step of simulated digestion. Here, the gastric chyme moves into the small intestine, where bile salts and pancreatic enzymes break down fats, proteins, and carbohydrates. In this phase, bile salts were prepared to reach a final concentration of 10 mM, while pancreatin was added to provide 100 U/mL of trypsin activity.

Bile Solution Calculation

To simulate the bile salt present in the small intestine during digestion, a final bile concentration of 10 mM was targeted in each 40 mL digestion volume.

Moles to mass requirements, given that the molar mass of bile salts is 408.6 g/mol.

$$Total\ Bile\ mass\ required = Moles * Molas\ mass \quad [5]$$

The minimum required mass was adjusted to 165 mg per sample. For eight samples, it resulted in a total stock mass requirement of 1,308 mg in 20.01 mL of SIF.

Pancreatin Calculation

Pancreatin was incorporated to mimic pancreatic enzymatic activity, with a target final activity of 100 U/mL in the total intestinal digestion volume of 40 mL per sample. Therefore, the target enzymatic activity per sample is 4000 U. The commercial enzyme used had a measured activity of 25 U/mg, the quantity of pancreatin needed per sample was 160 mg.

$$\frac{4{,}000\ U}{25\ U/mg} = 160\ mg \quad [6]$$

For the preparation of the pancreatin stock solution, 160 mg of pancreatin was dissolved in 5 mL OF Simulated Intestinal Fluid (SIF), resulting in a concentration of active pancreatin stock of 800 U/mL.

$$32\frac{mg}{mL} * 25\ U/mg = 800\ U/mL \quad [7]$$

To achieve the final pancreatin activity needed, 5 mL of the stock solution was added to each digestion tube, resulting in the intended 100 U/mL.

$$\frac{4{,}000\ U}{40\ mL} = 100\ U/mL \quad [8]$$

Then, for the preparation of 8 samples, 1280 mg of pancreatin were dissolved in 40 mL of SIF, introducing 5 mL into each sample tube.

Intestinal Digestion Process

Gastric chyme was diluted 1:1 (vol/vol) with simulated intestinal fluid (SIF). The composition of the simulated intestinal fluid is provided in Table 1, which lists the electrolyte solutions and stock concentrations used in this stage. Bile salts were added to a final concentration of 10 mM. Pancreatin was used at 100 U/mL trypsin activity, finally pH was adjusted to 7.0 using 5 M NaOH. Samples were incubated at 37 °C for 2 hours with continuous agitation (150 rpm).

Simulated Fluid Preparation

For each stage, simulated salivary fluid, simulated gastric fluid, and simulated intestinal fluid were used. Each was formulated with different proportions of the electrolyte stock solutions. The quantities of 250 mL for each fluid are detailed in table 2.

Table 2

Electrolyte solutions and stock concentrations for simulated fluids

Electrolyte added	Stock concentrations		SSF (pH 7)		SGF (pH 3)		SIF (pH 7)	
	(g/L)	(M)	mL stock / 0.4 L	(mM)	mL stock / 0.4 L	(mM)	mL stock / 0.4 L	(mM)
KCl	37.3	0.5	15.1	15.1	6.9	6.9	6.8	6.8
KH2PO4	68	0.5	3.7	3.7	0.9	0.9	0.8	0.8
NaHCO3	84	1	6.8	13.6	12.5	25	42.5	85
NaCl	117	2	-	-	11.8	47.2	9.6	38.4
MgCl2(H2O)6	30.5	0.15	0.5	0.15	0.4	0.12	1.1	0.33
(NH4)2CO3	48	0.5	0.06	0.06	0.5	0.5	-	-
HCl	-	1	0.09	1.1	1.3	15.6	0.7	8.4
CaCl2(H2O)2	44.1	0.3	0.025	1.5	0.005	0.15	0.04	0.6

Note. Table 2 details the preparation of three simulated digestive fluids: SSF (Simulated Salivary Fluid, pH 7), SGF (Simulated Gastric Fluid, pH 3), and SIF (Simulated Intestinal Fluid, pH 7). It shows the stock concentrations and volumes required to achieve the final electrolyte levels in 0.4 L of each medium.

Digestion

Following the intestinal phase, samples were then transferred from centrifuge tubes into dialysis bags. These bags were then subjected to a 48-hour digestion period to simulate the intestinal absorption phase, at 37 °C in constant motion in a surrounding medium (deionized water). The dialysis membranes, which act as semi-permeable barriers, allow for the diffusion of low molecular weight compounds, such as simple carbohydrates and sugars, into the deionized water medium. This duration facilitates the establishment of equilibrium between the interior of the dialysis bags and the external solution, mimicking the absorption of small molecules into the bloodstream within the small intestine.

Digested Samples Freeze Drying

Following the *in vitro* digestion process, each digested fiber sample was freeze-dried and pulverized. The digested material was transferred into 50 mL centrifuge tubes, with each sample

divided between two tubes to maximize surface area and improve water removal efficiency. The tubes were then stored overnight at –80 °C. On the following day, tubes were sealed with parafilm, perforated to allow moisture release, and placed in LABCONCO (2.5L) freeze dryer (pressure < 0.1 mbar) for 48 hours, or until complete moisture removal was achieved. Samples were subsequently ground to achieve a uniform pulverization of each fiber. This allowed a homogenous mixture when preparing the formulations of the fiber mixtures.

***In vitro* Anaerobic Fermentation**

Following upper GI digestion, the *in vitro* anaerobic fermentation phase was carried out to simulate colonic conditions and enable microbial metabolism of the digested substrates. This step was performed under strict anaerobic conditions to reflect the oxygen-free environment of the human colon, using a carbonate-phosphate buffer. The fermentation utilized a pooled fecal inoculum from two pediatric UC patients, providing a representative microbial community characteristic of UC-associated gut dysbiosis. The anaerobic fermentation procedure was conducted in BACTRONEZ® SHEL LAB anaerobic chamber from of Dr. Bruce Hamaker's Laboratory, following established internal protocols (Moncada et al., 2024).

Tube Requirement Calculations

The fermentation stage was designed to evaluate six different treatments across three timepoints (12 h, 24 h, and 48 h), each in triplicate, with an addition of six tubes for the 0-hour timepoint. The calculations for the total number of fermentation tubes were the sum of tubes per timepoint per triplicate plus the quantity of the 0-hour control tubes.

Tubes per Timepoint per Triplicate.

$$Triplicate\ Tubes = 6TRT * 3TMP * 3TRP = 54\ Tubes \quad [9]$$

Control tubes

$$0\ Hour\ Control\ Tubes = 6\ Tubes \quad [10]$$

Total number of tubes required was 60 tubes.

Total Buffer Volume Calculations

Each fermentation tube required a final volume of 5 mL per tube, with 4 mL of buffer volume, plus one additional mL of fecal slurry. To produce the fecal slurry, 1 gram of stool was mixed with 3 mL of buffer (1:3 ratio). For 60 tubes, 20 grams of stool were required (60 / 3 = 20 g), which were mixed with 60 mL of buffer. The total buffer needed was calculated based on the quantity of buffer required for the tube preparation, fecal slurry, and extra needed.

$$Total\ buffer = Tube\ buffer + Fecal\ Slurry\ Buffer + Extra\ Buffer \quad [11]$$

Buffer for Tubes were 240 mL. Buffer for Fecal Slurry were 6 mL. Additional Buffer (for rubber stoppers, rinses, and losses) were 200 mL. Total Buffer Required and Prepared was a total of 500 mL.

Preparation of Carbonate-Phosphate Buffer

To prepare for the *in vitro* fermentation procedure, the carbonate-phosphate buffer was prepared and introduced into the anaerobic chamber one day prior to fermentation, table 3 shows the stock concentrations for the preparation.

Table 3

Trace element solution and carbonate-phosphate buffer composition for 1L

Trace Element Solution		Buffer Composition	
mg/1000 mL		g/1000 mL	
FeSO4.7H2O	3680	NaHCO3	9.24
MnSO4.1H2O	1159	Na2HPO4	2.824
ZnSO4.7H20	440	NaCl	0.47
CoCl2.6H2O	120	KCl	0.45
NiCl2	100	Urea	0.4
CuSO4.5H2O	98	CaCla2.H2O	0.0728
Mo7(NH4)6O24.4H2O	17	Na2SO4	0.1
		MgCl.6H2O	0.1
		Trace Element Solution (mL)	10
		Resazurin (1 mg/mL)	1

Note. Table 3 presents the composition of the Trace Element Solution and the Carbonate-Phosphate Buffer used for in vitro fermentation. The trace element solution lists the amount of each compound (mg/L) needed to prepare 1 L, while the buffer composition indicates the concentration of each component (g/L) required for 1 L. The buffer also includes 10 mL of the trace element solution and 1 mL of resazurin (1 mg/mL) to complete the formulation.

For 500 mL of total buffer prepared, 494.5 mL of deionized water was used initially, allowing for the subsequent addition of 5 mL of trace element solution and 0.5 mL of a 0.1% resazurin solution, resulting in a final volume of 500 mL. The buffer was prepared by dissolving in the deionized water the components in reverse order of their listed concentrations, beginning with the minor components. This ensured dissolution and minimized precipitation. The solution was continuously stirred during the addition of each component. No heat was applied during this process to preserve buffer integrity.

After preparation, buffer filtration was made to ensure sterility. Prior to filtration, all components were confirmed to be completely dissolved to avoid filter clogging. Filtration was carried out using a vacuum system.

Following filtration, trace element solution and cysteine were added. Resazurin was prepared by dissolving 10 mg of resazurin in 10 mL of deionized water and stored at 4 °C until use.

Preparation of Fermentation Materials and Equipment

All materials that could come into direct contact with the fermentation samples, including labeled fermentation tubes, rubber stoppers, cheesecloth, pipette tips, rubber bands, spatulas, and beakers, were sterilized by autoclaving prior to the fermentation procedure. Additional materials required for the fermentation and data collection were also prepared in advance. These included tools for use inside the anaerobic chamber (pipettes, micropipettes, and scale), tools for use outside the chamber (metallic seal caps and cap crimper), as well as equipment such as the shaking incubator.

Preparation of Fiber Mixture Treatments

The fiber mixtures were formulated with five fibers for each fiber mixture, with one fiber repeated across mixtures. At this stage, the Anthocyanin Source Powder (AP) was also incorporated to enable direct evaluation of its potential interactions with the fiber matrices. A total of six treatments were assessed, as shown in table 4. However, due to confidentiality agreements, the

specific composition, both in terms of composition of the fiber formulations and anthocyanin concentration, cannot be disclosed. The table below outlines the treatments included in this phase of the study.

Table 4

Treatments assessed for anaerobic fermentation

	Treatment	Abbreviation
1	Blank	Blank
2	Fiber Mixture A	FMA
3	Fiber Mixture A + Anthocyanin Source Powder	FMA+AP
4	Fiber Mixture B	FMB
5	Fiber Mixture B + Anthocyanin Source Powder	FMB+AP
6	Anthocyanin Source Powder	AP

Note. Table 4 lists the six treatments evaluated during anaerobic fermentation. Each treatment is identified by its composition and abbreviation. A blank control, two fiber mixtures (A and B) tested individually and in combination with an anthocyanin source powder (AP), and one treatment containing only the anthocyanin powder.

A blank control was included in the experiment, consisting of only fermentation buffer and fecal inoculum, without the addition of any substrate. Additionally, for the treatment groups, each tube received 0.05 grams of the corresponding treatment as the substrate for fermentation.

Prior to the day of fermentation, 0.05 g of each fiber treatment was accurately weighed and added to individually labeled fermentation tubes. This step was carried out outside the anaerobic chamber. The blank control group did not receive any fiber treatment. After preparation, all tubes were transferred into the anaerobic chamber one day prior to the fermentation to flush oxygen and maintain anaerobic conditions.

Anaerobic Fermentation Process

On the day of fermentation, each tube was filled with 4 mL of carbonate-phosphate buffer inside the anaerobic chamber before inoculation with the fecal slurry.

Preparation of Fecal Slurry and Inoculation

Fecal slurry was made under anaerobic conditions according to laboratory protocol inside the anaerobic chamber (Moncada et al., 2024). Donor stool from two individuals was initially individually

frozen, thawed, and pooled by weight. During preparation, 20 grams of fecal material were used, obtained from 10 grams each from the donors. Inside the anaerobic chamber, the 20 grams of feces were combined with the previously calculated 60 mL of carbonate-phosphate buffer. The mixture was homogenized thoroughly using a sterile spatula. The homogenized fecal mixture was then filtered through three layers of sterilized cheesecloth, which had been secured over a beaker using an elastic rubber band. The filtrate was gently squeezed through the cloth to collect the fecal slurry. Subsequently, 1 mL of the fecal slurry was added to each fermentation tube. The tubes were then removed from the anaerobic chamber and sealed with metallic caps using a crimping machine.

Finally, the inoculated tubes were placed in a shaking incubator at 60 rpm and 37 °C for the fermentation process. Samples were then removed at the designated time points for subsequent analysis.

Data Collection

Preparation of Data Collection Materials and Equipment

At the time of data collection, all the required materials, as well as those for fermentation, were prepared in advance. The different forms of data they collected each required its own gear and equipment. Syringe displacement tests for gas production were conducted using hypodermic syringes and needles. For pH measurements, a calibrated benchtop pH meter was utilized, along with a decapper machine, vortex, and 15 mL centrifuge tubes. Additionally, 2 mL Eppendorf tubes were prepared for collecting samples intended for SCFA quantification.

Measurement of Gas Production

Gas accumulation was measured using a graduated glass syringe by inserting a 20-gauge needle through the rubber stopper of each fermentation tube, allowing the syringe to capture the gas generated in the headspace of the tube. Gas produced was determined by reading the displacement

indicated on the calibrated scale of the syringe. The tubes were then vortexed and opened using a decapper machine for pH measurement and sample collection for SCFA quantification.

pH Measurement

This parameter was measured with a benchtop pH meter to assess acidification in the fermentation process. The samples were transferred into 15 mL centrifuge tubes to measure pH. Subsequently, 1 mL of each sample was transferred into an Eppendorf tube, followed by storage at -80 °C for short-chain fatty acid (SCFA) determination.

SCFA Determination and Quantification

This step measures the metabolic outputs by comparing SCFA profiles amongst fiber mixtures alone and fiber plus anthocyanin treatments, evaluating how anthocyanins modulate fermentation pathways.

The frozen fermentation samples were thawed at room temperature. After thawing, samples were centrifuged at 13,000 rpm for 10 minutes to separate the supernatant from solid residues. 400 µL of the supernatant from each tube was carefully transferred into a gas chromatography (GC) vial (1.5 mL amber glass vial).

To ensure accurate quantification of short-chain fatty acids (SCFAs), an internal standard (IS) solution was prepared in advance. First, 157.5 µL of 4-methylvaleric acid was added to approximately 15 mL of deionized water. Then, 1.47 mL of 85% phosphoric acid was added to the solution and mixed to ensure homogeneity. Subsequently, 39 mg of copper (II) sulfate pentahydrate ($CuSO_4 \cdot 5H_2O$) was weighed and dissolved completely in the mixture. Finally, the volume was adjusted to a total of 25 mL using deionized water and mixed.

For each vial, 100 µL of the prepared internal standard solution was added. The vials were then vortexed for 5 seconds to ensure proper mixing and homogenization of the internal standard with the sample matrix.

The quantification of SCFAs was performed using a Hewlett-Packard (HP) 5890 Gas Chromatograph (GC) equipped with a flame ionization detector (FID). Separation of SCFAs was achieved using a Nukol capillary column (30 m × 0.25 mm internal diameter, 0.25 µm bonded phase; Supelco, Bellefonte, PA). Chromatographer conditions, including oven temperature, carrier gas flow rate, and detector settings, were set according to established: Supernatants (4 µl) were analyzed using a gas chromatography (GC-FID 7890A; Agilent Technologies Inc.) on a fused silica capillary column (NukonTM SUPELCO No: 40369-03A, Bellefonte, PA) under the following conditions: Injector temperature at 230 °C; initial oven temperature at 100 °C; temperature increase of 8 °C/min to 200 °C (Tuncil et al., 2018). The determined retention times are detailed in the table 5.

Table 5

SCFAs and their retention times

SCFA	Retention Time (min)
Acetic Acid	4.92
Propionic Acid	5.65
Isobutyric Acid	5.91
Butyric Acid	6.5
Isovaleric Acid	6.93
Internal Standard (Heptanoic Acid)	8.43

Note. Table 5 shows the short-chain fatty acids (SCFAs) identified by gas chromatography and their respective retention times (min). Acetic, propionic, isobutyric, butyric, and isovaleric acids were quantified, using heptanoic acid as the internal standard for calibration and normalization of results.

After GC analysis, SCFA concentrations were obtained by relating the areas of the obtained peaks to the calibration curves of the external standards. Concentrations are reported in Mm and are normalized relative to the internal standard. The data was processed with the Chromatography Data System software.

Experimental Design

The experimental design was designed to evaluate the effects of different dietary fiber and anthocyanin mixtures on fermentation parameters over time. The design used was a Completely Randomized Design with a two-factorial arrangement, to evaluate the effects of time and treatment

on the measured parameters. The study was structured to allow statistical evaluation of both individual treatment effects and their interaction with the specific timepoints, supporting broader application and reproducibility in other fermentation studies. These analyses were followed by the specifications and planning of PhD. student Paola Andino.

Treatment and Replicate Description

The experimental treatments consisted of six combinations of dietary fiber and anthocyanin sources, designed to investigate their impact on gut microbial fermentation, specifically targeting short-chain fatty acid (SCFA) production, gas output, and pH changes. In addition to the four experimental fiber mixtures with or without the anthocyanin source powder, a blank control (no added fiber) was included to establish baseline microbial activity under fermentation conditions, and a treatment with only the anthocyanin powder to assess its independent effects.

To establish a reference baseline for all outcome variables (gas production, pH, and SCFA concentration), samples were analyzed at time zero (0 h) prior to the fermentation process. This time point was analyzed using a single replicate per treatment to establish a baseline parameter for fermentation. For all other fermentation time points (21 h, 24 h, and 48 h), samples were analyzed in triplicate per treatment to ensure statistical reproducibility. This replication structure enabled the detection of treatment-time interactions and enhanced the precision of the estimated effects.

Data Analysis

A Completely Randomized Design (CRD) was employed to assess measures influenced by treatments over time. Figure 1 and figure 2 outline the data analysis flow for all datasets and parameters, including analyses with both normal and non-normal distributions.

Figure 1

Data analysis diagram for data with a normal distribution

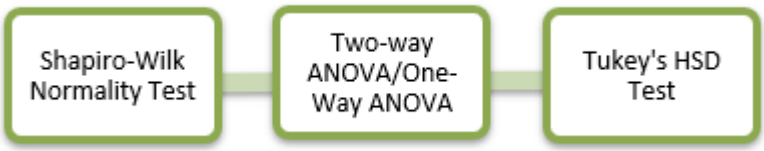

Note. Figure 1 describes the statistical analysis workflow. Data were first evaluated for normality using the Shapiro–Wilk test, followed by one-way or two-way ANOVA to determine significant differences among treatments. When significant effects were detected, Tukey's HSD test was applied for mean separation.

A Shapiro-Wilk normality test was conducted for all datasets to indicate the presence of a normal distribution. When data deviated from normality, logarithmic transformations were applied prior to further analysis.

Figure 2

Data analysis diagram for data with a non-normal distribution

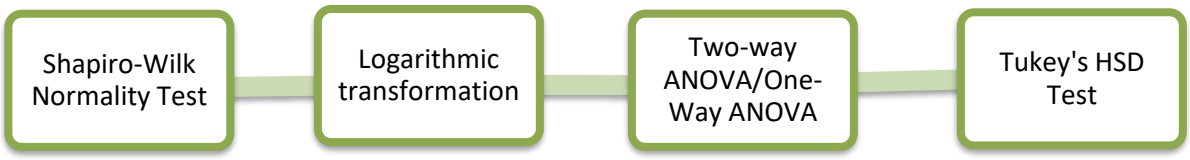

Note. Figure 2 describes the statistical analysis workflow with data transformation. When data deviated from normality, a logarithmic transformation was applied prior to conducting ANOVA and Tukey's HSD tests to ensure validity of the statistical assumptions.

A Two-Way Analysis of Variance (ANOVA) was used to evaluate the main effects of treatment and time, as well as their interaction, on gas production, pH, and SCFA concentrations. This type of analysis was used for assessing repeated measures across different treatment groups over time.

Fermentation efficiency of butyrate and SCFAs, calculated as the ratio of mM of butyrate and SCFA produced per mL of gas, was analyzed at the last time point. This analysis was performed using a One-Way ANOVA, and its purpose was to highlight the treatment that maximized SCFA and butyrate production in relation to gas production.

Tukey's Honestly Significant Difference (HSD) post-hoc test was performed following all ANOVA procedures to determine statistically significant differences between individual groups. Significant differences were established at $p<0.05$, reported using alphabetical superscripts.

Bliss Synergy Calculation.

To determine synergy between the two fiber mixtures and the anthocyanins, Bliss Synergy independence was calculated. This model assumes that two compounds act independently, so their combined effect can be predicted as the sum of their individual fractional effects minus their product (Foucquier y Guedj, 2015). When the observed combination effect is compared with this expected value, the difference, known as Excess-over-Bliss, allows classification of the interaction as synergistic, additive, or antagonistic (Demidenko y Miller, 2019; Zhao et al., 2014). Because this approach requires fractional effects, raw data were normalized to a 0–1 scale to make comparisons valid across treatments (GraphPad Software, 2024).

Synergy between fiber and anthocyanins was evaluated using the Bliss independence model, which is based on the principle that two agents acting independently should produce a combined effect equal to the sum of their individual fractional effects minus their product (Greco et al., 1995; Zhao et al., 2014). This model allows the expected additive effect to be calculated mathematically as:

$$E = Fa + Fb - (Fa * Fb) \quad [12]$$

Where Fa and Fb represent the normalized fractional effects of the fiber and anthocyanin treatments, respectively, and E is the expected effect under additivity. Furthermore, observed effects of the fiber–anthocyanin combination (O) were then compared with the expected Bliss value (E) to obtain the Excess-over-Bliss score:

$$\Delta = O - E \quad [13]$$

Positive Δ Values indicate synergy, values close to zero indicate additivity, and negative values indicate antagonism. This framework is commonly used to assess interactions between bioactive compounds because it assumes statistical independence.

In order to enable comparisons between treatments, data were normalized to fractional effects ranging from 0 to 1, such that the mean of the lowest group was set at 1, according to the instructions of GraphPad Prism for the Normalize analysis (GraphPad Software, 2024). Normalization was important because Bliss calculations are performed on fractions rather than raw values of effects. Finally, Excess over Bliss values were subjected to statistical analyses. T-tests one-sample versus zero were performed on the Δ values in order to test for significant deviations from the expectation of no interaction, as is standard practice.

When the test indicated significance ($P < 0.05$), the interaction was considered either synergistic ($\Delta > 0$) or antagonistic ($\Delta < 0$).

Results and Discussion

Parameters were quantified or calculated to allow for greater insight into fermentation results. Outcomes assessed include pH, gas production, butyrate, and SCFA levels and composition. Parameters calculated include butyrate production efficiency, SCFA production efficiency, and synergy as determined by Bliss independence.

pH

The pH changes observed across the treatments measure acidification through fermentation, where microbes break down available substrates and produce metabolites over time. These are mainly acids and SCFA, which cause a drop in pH (Deehan et al., 2017). In the current study, the treatments that included fermentable substrates illustrated a standard behavior of microbial fermentation with the observed decline of pH over time.

Figure 3 shows the behavior of pH throughout the fermentation process. This measurement revealed the main differences in acidification, with the blank control showing the lowest, FMA treatments medium, and FMB treatments, along with AP, showing greater acidification. The pH drop between 0 and 12 hours was higher for the FMB treatments. Suggesting that the FMB treatments are more fermentable and would favor the rapid production of SCFAs (Feng et al., 2022).

However, for UC conditions, this overproduction of acids in a short amount of time is associated with unrestricted fermentation in the colon, which could be disruptive for the epithelial cells (Nemzer et al., 2025). FMB+AP showed a slower decline in pH, and at 48 hours, its pH was similar to that of FMB groups and AP. Such a delay in pH lowering suggests that the anthocyanin-fiber complexes influenced a slower acidification (Sejbuk, Mirończuk-Chodakowska, et al., 2024).

Figure 3

pH changes over time

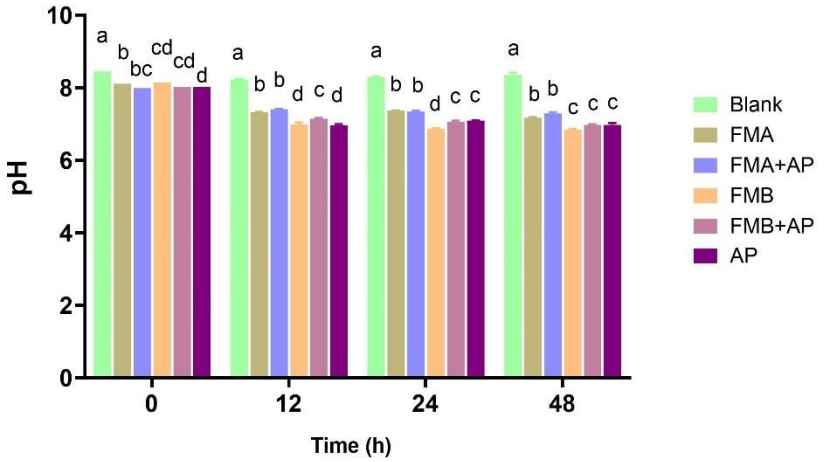

Note. Figure 3 shows pH changes during *in vitro* fecal fermentation, monitored across all time points (0, 12, 24, and 48 h). The blank served as the negative control, and each treatment was performed in triplicate (n = 3) at every time point. Different letters above the bars indicate statistically significant differences among treatments at the same time point ($p < 0.05$).

However, FMA and FMA+AP showed moderate acidification. This can be explained by the higher number of insoluble fractions in FMA treatments. According to Pirkola et al. (2023), higher insolubility in fibers is correlated with lower fermentation capacity and acid formation, resulting in a reduced decrease in pH.

It is crucial to explain that pH, especially in UC conditions, is not by itself a measure of effectiveness in SCFA production. In conditions of dysbiosis, SCFA producers are reduced, resulting in lower SCFA production, which could translate into lower acidification (Gillis et al., 2018). However, acidification can also occur due to production of lactate or succinate, rather than an increase of SCFA (Ma et al., 2017). This is more recurrent in UC because dysbiotic microbiota leads to reduced lactate cross-feeders. Consequently, lactate lowers pH sharply without providing the same benefits and SCFA profiles as those from sustained acidification (Ozdal et al., 2016). Additionally, *in vivo* studies associate lower pH with active and flares in UC Therefore, pH must be interpreted alongside metabolite profiles to determine a better fermentation capacity (Bai et al., 2016).

Gas Production

Gas production during fermentation is indicative of the activity of gut microbes in degrading carbohydrates. These substrates are fermented by these bacteria, resulting in the production of gases such as hydrogen, and carbon dioxide (Makki et al., 2018). These gases are generated as byproducts of this process; their production is dependent on the pathway of consumption of hydrogen by microbes (Valles-Colomer et al., 2019). However, in the case of UC, high and rapid gas production is associated with exacerbation of gastrointestinal distress and distension (Aliu et al., 2024).

The gas production per treatment over time (Figure 4) shows that the blank control was consistently the lowest, FMA treatments resulted in a significantly lower amount of gas, compared to FMB+AP and AP which were higher and FMB that yielded the highest overall value. Firstly, these pathways leading to increased gas production in FMB treatments compared to FMA treatments are due to differences in the type of fibers in their composition (Dell'Olio et al., 2024). Because fibers in FMB are faster fermentable, they generate higher and earlier gas than the slower ones (Gunn et al., 2022). Faster fiber fermentation is believed to be driven by factors such as chain length, types of microorganisms present, viscosity, and solubility (H. Li et al., 2020; Wang et al., 2019). However, solubility, which was usually linked to faster fermentation, has been demonstrated not to be a great indicator of fermentability speed (Mutuyemungu et al., 2023). Because insoluble fibers reported the same fermentation speed as soluble fibers in a study by Moncada et al. (2024).

Figure 4

Gas production over time

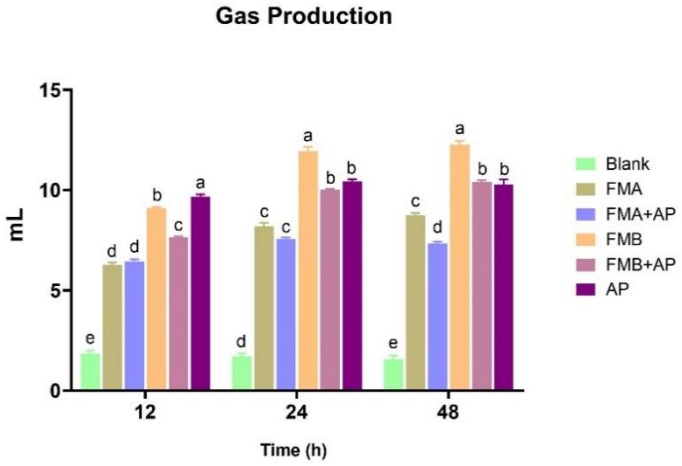

Note. Figure 4 indicates the amount of gas produced (mL), recorded at 12, 24, and 48 h during in vitro fecal fermentation. The blank was included as the negative control, and all treatments were tested in triplicate (n = 3) at each time point. Bars labeled with different letters indicate significant differences among treatments in the same time point ($p < 0.05$).

The fiber-only treatments yielded higher gas production compared to the same fiber mixtures containing anthocyanins. At 12 and 24 hours, FMA was statistically similar to FMA+AP, but at 48 hours, it began to increase above the level of the other treatment. FMB+AP was also less gas-producing than FMB at all time points. A similar pattern was observed in a study by Campbell et al. (2023), where the combination of anthocyanins and dietary fiber resulted in lower gas production due to the stimulation of pathways that use hydrogen, reducing its accumulation (Ray y Mukherjee, 2021). Several factors influence these outcomes. As demonstrated by Y. Zhang et al. (2025), High Amylose-anthocyanin complexes had the capacity to lower the redox potential of the fermentative system (Raj et al., 2010).This favors strict anaerobes, which convert H2 to acetate. This decreases H2 (gas) build-up, ultimately enhancing cross-feeding to the butyrate producers (Bui et al., 2019). This is favorable for UC patients, who would benefit from less pronounced gas accumulation peaks (Staudacher et al., 2014).

Total SCFA Production

SCFAs are the main end products of fermentation (Ziętek et al., 2021). Among all SCFAs, butyrate, acetate, and propionate are usually the ones in major concentrations, and they mainly serve as an energy source for colonocytes. They also help protect the intestinal barrier, modulate inflammation, and maintain microbial homeostasis (Canfora et al., 2019; Louis y Flint, 2017). These characteristics are useful for conditions like UC (Parada Venegas et al., 2019).

As observed in Figure 5, the blank treatment remained low in SCFA levels at all time points. FMB applications induced the highest SCFA, followed by FMA. The present findings indicated that supplementation with anthocyanins was not superior for SCFAs compared to the fiber treatments. It has been reported that dietary polyphenols, including anthocyanins, can influence both redox potential and the balance of microbial populations, favoring SCFA-producing taxa (Pasinetti et al., 2018). Still, in this case, no variations were found among fiber blends or fiber mixes plus anthocyanin combinations. This restriction of anthocyanin activity can be attributed to UC dysbiosis, where reduced microbial diversity is a limiting factor (Cosier et al., 2024). This condition reduces richness and lowers the abundance of taxa with anti-inflammatory functions in pediatric UC, including saccharolytic genera that produce SCFAs (Putignani et al., 2021). Then, for this study, the most relevant factors influencing higher or lower SCFA production were the structural properties and the chemistry of the fiber mixtures themselves (Hamaker y Cantu-Jungles, 2020).

Figure 5

Total SCFA production

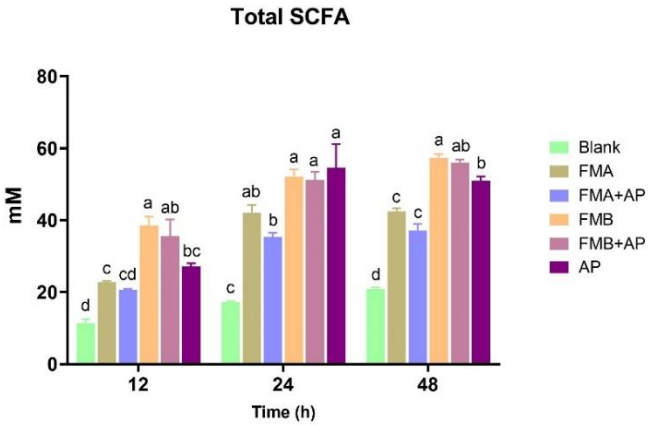

Note. Figure 5 shows total short-chain fatty acid (SCFA) concentrations (mM). Each treatment was evaluated in triplicate (n = 3), and the blank served as the negative control. Distinct letters above the bars indicate statistically significant differences across treatments for the same measurement ($p < 0.05$).

In this sense, the physicochemical properties of the fibers determined the differences in SCFA production among treatments. Firstly, solubility is an important factor for determining microbial utilization and SCFA production (Xu et al., 2021). Treatments with FMB had a higher solubility, which makes them hydrate more effectively than FMA treatments. A study by Y. Bai et al. (2021) investigated the effects of fiber type and source on the production of SCFA. Here, they linked higher solubility to more accessible glycosidic linkages. Where microbial carbohydrate-active enzymes (CAZymes) were able to break down the substrate more effectively. This interaction improves the rate at which mono- and oligosaccharides are released and then metabolized into SCFAs (Thilavech et al., 2025). In this context, higher solubility in FMB treatments played a role in faster microbial access and greater total SCFA production compared to FMA mixtures. Less soluble fibers require more specialized mechanisms for microbial degradation, which leads to lower SCFA production (Cantu-Jungles et al., 2021).

In addition, the complexity of the structures also plays an important role in SCFA production. According to Cantu-Jungles et al. (2019), fibers differ in branching, linkage types, and side-chain decorations. Through this, the influence of these characteristics decides which microbial taxa can metabolize the substrate, because enzymes recognize specific linkages. For example, arabinoxylans

that differ in their arabinose substitution patterns can yield distinct SCFA profiles, because only certain microbes possess the enzymes to break down those linkages (Hamaker y Cantu-Jungles, 2020). Moreover, Louis et al. (2021) found that fiber structures with diverse branching and mixed glycosidic linkages promote the growth of diverse microbes. This allows simultaneous saccharolysis and cross-feeding, resulting in more accessible substrate for SCFA producers. On the other hand, the simpler structures of FMA treatments may have reduced substrate variety and availability for microbial cross-feeding (Williams et al., 2019).

SCFA Production Efficiency

SCFA production efficiency is used to assess the effectiveness of fermentation, showing the total volume of SCFAs produced in millimolar per milliliter of gas. It helps measure how much valuable target compounds in colonic fermentation under UC conditions, such as SCFAs, are produced in relation to the gaseous co-products that accumulate and relate to bloating, such as H2, CO2, and CH4 (Y. Bai et al., 2021).

According to Figure 6, almost all treatments were equally efficient in SCFA production efficiency. The only two treatments that differed statistically were FMB+AP (a) and FMB (b).

The lower efficiency in FMB is in accordance with its soluble and faster fermentable fiber content. These features make the substrate more accessible to microorganisms and lead to an earlier rise in total gas production (Tuncil et al., 2018). On the other hand, the FMB+AP difference with FMB indicates that the combined use of anthocyanin powder enhanced the efficiency of SCFA production by fiber-polyphenol interaction (Kapoor et al., 2023). Upon reaching the colon, these anthocyanins are further metabolized by bacteria into small phenolic acids, including protocatechuic, vanillic, syringic, and p-coumaric acids (Li et al., 2020). These compounds donate electrons during microbial metabolism, which makes them able to scavenge reactive oxygen species and lower the redox potential (Kumar y Goel, 2019). This reduced environment favors acetogenesis over methanogenesis because acetogens require strong reducing conditions to convert H2 and CO2 into acetyl-CoA, which

is later turned into acetate (Campbell et al., 2023). This promotes the growth of beneficial bacteria and reduces opportunistic or pathogenic bacteria, which often produce more gas relative to SCFAs (Kapoor et al., 2023). This is favored by fermentable fibers, which act as a substrate. A review by Cheng et al. (2025) identified that fibers (by acting as a fermentable substrate), along with anthocyanins (which act as fermentation modulators), together enhance SCFA-producing bacteria. In this context, Fernandes et al. (2023) reported that the physicochemical properties of fiber, including water holding capacity, viscosity, microstructure, and fermentability, modulate fiber-polyphenol interactions in relation to the promotion of SCFA production while controlling gas production.

Figure 6

SCFA production efficiency (mM of SCFA/mL gas)

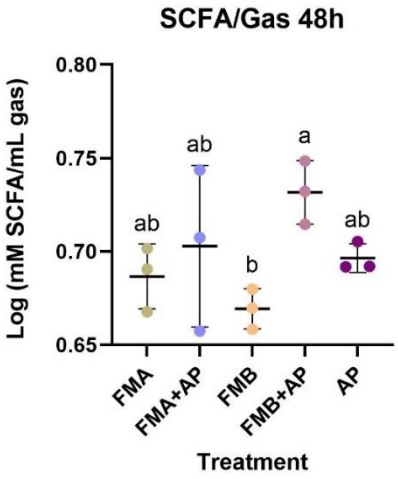

Note. Figure 6. SCFA production efficiency at the time point, expressed as mM of SCFAs per mL of gas. Data was log-transformed to correct for non-normal distributions observed in one treatment. Triplicates (n = 3) were included for all treatments, and different letters indicate statistically significant differences among them ($p < 0.05$).

Additionally, according to studies, anthocyanins shift microbial communities to communities that promote conversion from hydrogen to acetate. Hydrogen is produced during fermentation, which may accumulate or be converted into methane (Kapoor et al., 2023). However, anthocyanins promote taxa that scavenge H2 and CO2 to produce acetate that reduces H2 (gas) buildup. This provides available substrate to butyrate producers (Campbell et al., 2023).

SCFA Composition

The total SCFA composition indicates how metabolite production patterns occur across time points during fermentation (Van-Wehle y Vital, 2024). As shown in Figure 7 and supported by Appendix 4, at 48 hours FMB+AP managed to increase butyrate percentage higher than FMB. The rise in butyrate percentage reflects how anthocyanins and fibers interact with the gut microbiota. Anthocyanins promote cross-feeding, where acetogens supply acetate that butyrate producers convert into butyrate, raising its share in the SCFA profile (Park et al., 2024). Some studies claim fiber type is also important, since pectin or β-glucan change how anthocyanins are metabolized and shape fermentation patterns that favor butyrate pathways (Yang et al., 2021)

Moreover, the rise in butyrate and propionate percentages in all treatments from 12 to 48 hours is proportional to the decline in acetate. Acetate is the most prevalent of the SCFAs since it is produced by primary fermentation and serves as a precursor for the production of both butyrate and propionate (Mocanu y Madsen, 2024). Butyrate generation is explained by the acetyl-CoA pathway, in which acetate is consumed by butyryl-CoA: acetate CoA-transferase to release butyrate, which explains why acetate can decrease in relative proportion as butyrate rises (Noguer et al., 2022). Additionally, propionate is increased through the succinate pathway, to transform propionyl-CoA with succinate or acetate to form propionate. This reduces the acetate concentration by fermentation and increases the concentration of propionate (Döring y Basen, 2024).

In this sense, the higher complexity through branching, viscosity, and solubility of FMB treatments may have favored the growth of cross-feeders. These are associated with soluble structures that produce propionate through the succinate pathway (Louis et al., 2021). Furthermore, a study by Jalanka et al. (2019) compared various dietary fibers and found that psyllium fiber (a soluble and gel-forming fiber) significantly promoted *Bacteroidetes.* This was linked with an increase in propionate production. Thus, the characteristics of FMB are more consistent with those in that study.

Figure 7

Total SCFA Composition at 12 and 48 hours

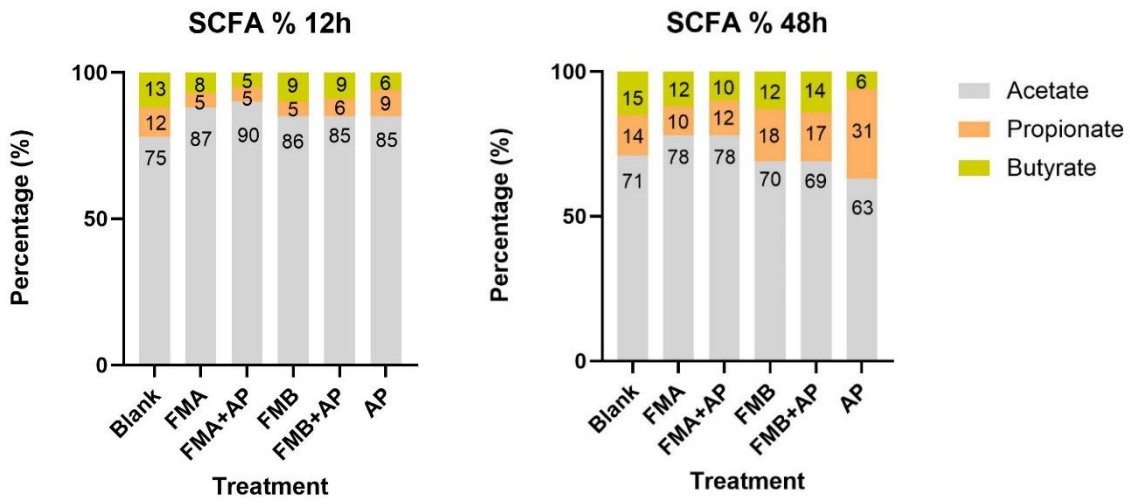

Note. Total SCFA composition is shown as the percentage contribution of acetate, propionate, and butyrate for each treatment. Results are presented at both 12-hour and 48-hour fermentation time points. Statistics for this figure are shown in Appendices 4 & 5.

For the AP treatment, the SCFA profile at 48 hours induced a higher increase in propionate compared to the other treatments, as indicated in Appendix 4. Previous studies indicate that anthocyanins support the growth of butyrate-producing bacteria. This results in increased levels of butyrate both in *in vitro* and *in vivo* models (Lopez-Siles et al., 2018; Sejbuk, Siebieszuk & Witkowska, 2024) However, it has also been demonstrated that the effect of polyphenols on modulating microbiota is influenced by the dose and the substrate it is paired with. Anthocyanins can change the balance of the gut community in a way that favors propionate under certain conditions (Zhu et al., 2022). Its food matrix for example, blackcurrant has a xyloglucan-rich fiber and polyphenol complex that is easier for *Bacteroidia* to use, especially at the start of fermentation, pushing metabolism toward propionate (Döring y Basen, 2024).

Butyrate Production

Butyrate is especially important in UC because it is the main energy source for colonocytes. This, along with its studied effects of strengthening the gut barrier and reducing inflammation (Parada

Venegas et al., 2019). In people with UC, especially pediatric patients, butyrate-producing bacteria are often reduced in number. This leads to lower butyrate levels and a weaker epithelial defense. Restoring butyrate production can help improve barrier integrity, regulate immune responses, and ease inflammation (Maiuolo et al., 2024; Singh et al., 2022)

Figure 8 indicates that FMB produced butyrate at the highest quantities since the beginning. While FMB+AP produced less butyrate than FMB at 12 and 24 hours, it reached the same level by 48 hours. This slower rise in FMB+AP is attributed to the interaction of anthocyanins and fibers. Anthocyanins are converted into phenolic acids, which serve as alternative electron acceptors while decreasing redox potential and preventing H2 accumulation. This property delays butyrate production and promotes it at later time points (Parada Venegas et al., 2019; Rodríguez-Daza et al., 2021). This is more advantageous in a UC-type environment since low levels of butyrate and redox imbalance are typically found (Muro et al., 2024). A slower release of butyrate assists in epithelium energy flow and anti-inflammatory signaling in the distal colon, the target area in UC (Singh et al., 2022). Therefore, while FMB alone gave a faster increase, the delayed but sustained effect of FMB+AP could be advantageous in this disease context.

Figure 6

Butyrate production

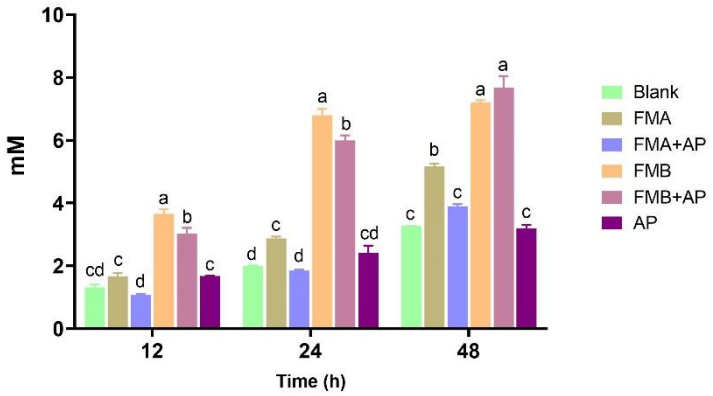

Note. Figure 8 shows butyrate production in mM, measured throughout fermentation. Each treatment was tested in triplicate (n = 3), and different letters above the bars indicate significant differences among treatments at the same time point ($p < 0.05$).

When anthocyanins were added to FMA+AP, the production of butyrate was reduced at all time points. This finding can be supported by a study by Shi et al. (2024), which discussed the interaction among fibers and anthocyanins through non-covalent (such as hydrogen-bonding and electrostatic forces) and covalent bonding. These types of interactions influence positively or negatively the outcomes of fermentation.

Butyrate Production Efficiency

In this study, butyrate production efficiency means the amount of butyrate produced per milliliter of gas. This ratio helps identify the treatment that yields the most beneficial metabolite (butyrate) with the least by-product (gas). This is important in UC specifically, as butyrate promotes the health of the colon lining and reduces inflammation, while excess gas is one factor associated with worsened symptomology (Singh et al., 2022).

Figure 9 reveals that FMB+AP was the most efficient. The positive interaction of fiber-anthocyanin can be explained by the type of bond FMB's characteristics promoted. For instance, non-covalent bonds retain anthocyanins within the fiber matrix; however, unlike covalent bonds, they are reversible and help the gradual release of anthocyanins during colonic fermentation (Fernández-Veledo et al., 2025). This interaction has been extensively studied for low-methoxyl pectins, as their carboxylate groups and hydroxyls enable non-covalent interactions with the flavylum form of anthocyanins at acidic pH (Shi et al., 2024). Furthermore, these types of bonds have been implicated to be affected by viscosity, which is linked to lower early gas and distal metabolite production (Harris et al., 2023)This interaction is beneficial for UC symptoms, where viscous fibers can contribute to the gradual delivery of butyrate. This distal delivery to the colon is more beneficial for UC symptoms (Recharla et al., 2023).

Figure 7

Butyrate production efficiency (mM Butyrate/mL gas)

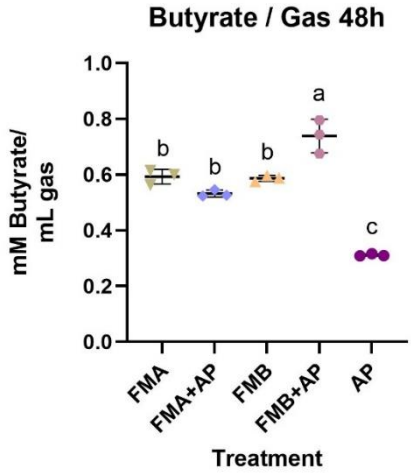

Note. Figure 9. Butyrate production efficiency at the 48-hour time point is expressed as mM of butyrate per mL of gas. The blank acted as the negative control, and all treatments were performed in triplicate (n = 3). Statistical differences among treatments are indicated by different letters ($p < 0.05$).

In contrast, FMA, FMA+AP, and FMB alone showed similar efficiency. This indicates that their structures did not provide additional advantages beyond the general fermentation of fibers. FMA may have limited accessibility for butyrate producers. This reduces the potential for efficient cross-feeding and butyrate yield (Tuncil et al., 2018). AP alone was the lowest in efficiency, which was expected because it promoted the production of propionate alone rather than butyrate.

Overall, this high efficiency observed in FMB+AP compared to all other treatments suggests a possible synergy between the fiber mixture B and anthocyanins. The synergy calculation determines whether this combined effect (FMB+AP) outperforms both FMB and AP alone in producing more butyrate in the minimum amount of gas possible.

Synergy (Calculated by Excess Over Bliss)

To determine synergy between the two fiber mixtures and the anthocyanins, Bliss Synergy independence was calculated. This model assumes that two compounds act independently, so their combined effect can be predicted as the sum of their individual fractional effects minus their product

(Foucquier y Guedj, 2015). When the observed combination effect is compared with the expected value, the difference, known as Excess-over-Bliss, allows for the classification of the interaction as synergistic, additive, or antagonistic (Demidenko y Miller, 2019).

According to Figure 10 and Table 6, the combination of FMB with the AP resulted in a synergistic effect on butyrate production efficiency ($\Delta = 0.3547 > 0$) & (p=0.046<0.05). In contrast, FMA treatments did not significantly differ from zero; therefore, they produced an additive effect ($\Delta = -0.2169 < 0$) & (p=0.1091>0.05). This indicates that the structural characteristics of FMB synergized with anthocyanins to increase fermentation efficiency toward the same amount of butyrate with less gas.

To illustrate these results, it has been previously shown that the stabilization of anthocyanins occurs through complexes with soluble and more viscous fibers, such as those present in FMB (He et al., 2023; Hou et al., 2022). Higher viscosity is associated with higher molecular weight, increased numbers of hydroxyl groups, and the presence of ionizable carboxyl groups (Dikeman & Fahey, 2006). These more available functional groups also mediate direct binding with anthocyanins. Phenolic hydroxyls of anthocyanins can bond with hydroxyl (-OH) and carboxyl (-COO-) groups of polysaccharides (Koh et al., 2020; Larsen et al., 2019). These non-covalent bonds strengthen anthocyanin holding capacity, retaining and dispersing anthocyanins for longer, enabling a sustained colonic release. Solubility is highly linked to viscosity, since soluble fiber matrices have water-binding hydroxyl groups and lead to viscous and gel structures (Lante et al., 2023). Viscosity has been shown to physically allow for the adhesion of anthocyanins to the fiber molecule, establishing a more durable stickiness and further extending substrate availability during fermentation (Huo et al., 2025; Requena et al., 2018). On the contrary, extremely high viscosity of a fiber matrix can also limit the release of compounds and the accessibility of the anthocyanins (Jakobek et al., 2022). Then, an optimal equilibrium must be found to achieve fermentation that minimizes gas formation while maintaining or increasing butyrate levels. Besides, it is also worth noting that solubility is not always accurate for

determining fermentation rate, particularly under UC conditions. This is because some insoluble fibers can produce equal or greater amounts of SCFAs and gas than soluble fibers, depending on their structure and microbial interactions (Moncada et al., 2024).

Moreover, Fernandes et al. (2023) noted that the degree of methylation of pectin affects both chemical interaction and fermentation behavior. Lower methoxyl pectins have more free carboxylate groups, which bind strongly with calcium ions, forming cohesive gels. These complexes strengthen electrostatic and hydrogen-bond contacts with the cationic flavylium forms of anthocyanins during digestion (Fu et al., 2023). This increases stability in a food matrix and promotes sustained fermentation (Shi et al., 2024). Thereby, pectin present in the AP matrix may have further helped this interaction.

Figure 8

Excess over Bliss calculation graph

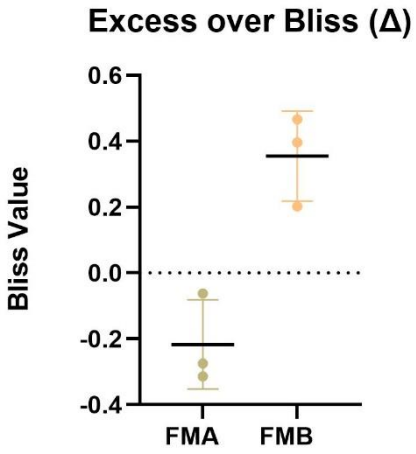

Note. Figure 10 shows synergistic interactions calculated using the excess over Bliss independence model. Values above 0 indicate synergistic effects, whereas values below 0 indicate antagonism. Treatments were run in triplicate (n = 3). However, the Bliss model uses normalized data for determining the domain of a treatment. Therefore, a treatment can include 0 in its domain regardless of how this graph displays it. Analyze Table 6 for determining any synergistic effect.

Table 6

T-test analysis for Excess Over Bliss Synergy calculation

Treatment	Actual mean Δ (±SEM)	n	t (df)	95% CI of Δ	P value	Significant vs 0 (α=0.05)
FMB + AP	0.3547 ± 0.079	3	t = 4.490 (df=2)	0.01480 to 0.6946	p = 0.0462	Yes
FMA + AP	-0.2169± 0.07818	3	t = 2.774 (df=2)	-0.5533 to 0.1195	p = 0.1091	No

*Note. Table 6 describes the results of the s*tatistical analysis of Bliss Independence by Excess Over Bliss. It includes the treatment means, standard errors, sample sizes, t-values, confidence intervals, and p-values. Here, significance is judged at α = 0.05: values below this threshold indicate a difference from zero. When Δ is positive and significant, the effect is synergistic; when it is not significant, it suggests an additive effect; and when Δ is negative, it reflects an antagonistic interaction.

Redox potential is another factor that indirectly influences lower gas accumulation in treatments with anthocyanins. This supported the synergistic effect in FMB+AP. Under UC conditions, the inflamed lining leaks oxygen into the lumen and oxidizes the gut. This condition favors dysbiosis by allowing non-obligatory anaerobe bacteria to flourish instead of butyrate cross-feeders (Quaglio et al., 2022). Furthermore, more recent *in vitro* studies have shown that anthocyanins reduce the redox potential of fiber fermentation, with implications on increased butyrate levels (Zhang et al., 2025). Anthocyanins are broken down into simpler metabolites, and they act as electron acceptors and thus lower the redox potential of the gut. As a result, these compounds reduce this system, leaving optimal environments for anaerobic bacteria such as acetogens, sulfate reducers, butyrate, and propionate cross-feeders (Rodríguez-Daza et al., 2021; Schoelmerich & Müller, 2020). This indirectly promotes hydrogen instead of gas accumulation. Hence, the enrichment with anthocyanins under reduced conditions promotes the cross-feeding of anaerobes.

Overall, the mechanisms described are in accordance with the positive results for FMB+AP, indicating its synergistic effect on butyrate production efficiency. These mechanisms become favorable for alleviating symptoms in UC dysbiosis, where patients experience fiber intolerance (Armstrong et al., 2023). In UC, the reduction in butyrate production weakens the gut barrier, promoting inflammation that manifests as pain, bloating, swelling, diarrhea, among others

(Ungaro et al., 2017). Dysbiosis promotes the metabolism of microbes to irritant gases and oxidative stress, in which hydrogen sulfide can damage the gut lining and promote swelling and ulceration (Stummer et al., 2023). Besides, metabolite accumulation, such as hydrogen or succinate, can contribute to bloating and activate inflammatory markers such as SUCNR1 and NF-κb (Huo et al., 2025). The FMB+AP treatment managed to restrain gas production while still supporting SCFA production by cross-feeding (Bui et al., 2019). Plus, the ability of the anthocyanins to decrease redox potential also supported a reduced environment dominated by strict anaerobes. Previous studies also suggest that gel-forming fibers use FXR signaling to exert anti-inflammatory action (Bretin et al., 2023).

Microbial profiling (Complementary Data to this Study)

Microbial profiling was carried out subsequently to this study by PhD. Purdue Student Paola Andino and was therefore not included in the experimental design. Then, this section discloses microbial profiling to support the results of the study. The graphics discussed are annexed in the appendices.

This process identifies which bacteria are present in a sample and in what proportions, analyzed through sequencing techniques, in this case, 16S rRNA (Quince et al., 2017).

Shannon entropy, according to Appendices 1 and 2, showed that the blank had the highest diversity, however, diversity index is not a reliable success metric in dietary interventions (Thaisa M. Cantu-Jungles et al., 2019). Since the families driving this diversity, such as *Finegoldia* and *Peptoniphilus*, are linked to UC dysbiosis and thrive when inflammation increases oxygen and nitrate in the gut (Baldelli et al., 2021; Byndloss et al., 2017; Litvak et al., 2018). At 24 hours, both FMB and FMB+AP had lower diversity, which agrees with earlier reports showing that primary fermenters dominate at the start and reduce evenness (Hamaker y Tuncil, 2014; Sugihara y Kamada, 2021). Moreover, by 48 hours, FMB+AP (a) increased in richness, along with FMB (b). This change reflects that the selected fibers plus fiber-anthocyanins benefited cross-feeding bacteria at a sustained rate. With primary fermenters supplying substrate for secondary butyrate producers (Azad et al., 2018).

According to genus relative abundance (Appendix 3), the changes in specific taxa confirmed the patterns described before. *Escherichia* remained lower in FMB treatments than in FMA treatments. This indicates that FMB fiber composition suppressed the growth of this facultative anaerobe (Arthur et al., 2012; Winter & Bäumler, 2014). In addition, *Streptococcus,* a facultative lactate fermenter, increased in FMB and decreased in FMB+AP from 24 hours to 48 hours. The same decreased behavior is observed with the primary lactate and acetate fermenter, *Fusicatenibacter*. This suggests that the presence of anthocyanins favored the conversion from lactate to propionate at the 48-hour timepoint (Nishino et al., 2018; Takahashi et al., 2016). This statement is further supported by the slightly higher increase of FMB+AP compared to FMB, in the propionate fermenter *Bacteroides.* This, along with the butyrate fermenters, *Clostridium and Blautia* (Do et al., 2023).

In combination, FMB+AP induced a slight reduction in *Streptococcus* and *Fusicatenibacter*, bacteria that produce lactate and acetate that can be cross-fed, and *Escherichia,* an active gas producer (Li et al., 2024). FMB+AP also induced a slightly higher increase in cross-feeders, *Blautia, Clostridium,* and *Bacteroides*, compared to FMB. Altogether, the microbiota influenced by FMB+AP explain the measured higher SCFA and butyrate production efficiency compared to FMB. These findings show a trend in microbial composition. This suggests the capacity of the fibers in FMB to synergize with anthocyanins, producing the same quantities of butyrate and SCFA in less gas. This, while promoting beneficial taxa associated with remission in UC, and reducing taxa associated with gas production, compared to the control (Heinzel et al., 2024; Jangi et al., 2025). (Mutaz, 2024)

Conclusions

This study found that dietary fibers can synergize with anthocyanins to offer an advantage in butyrate production with reduced gas production under UC dysbiosis. When used together, they created a sustained secondary metabolite production, which is important because excessive gas is a common symptom of discomfort in UC, while butyrate plays a crucial role in protecting and repairing the gut lining.

Additionally, this study emphasizes the influence of the physicochemical characteristics and fiber type to achieve more favorable outcomes in UC. FMB treatments reached a more optimal equilibrium in terms of solubility, complexity, and viscosity. These characteristics favored the interaction between fiber and anthocyanin, allowing for a more controlled fermentation process with the same levels of butyrate produced, but in a smaller amount of gas.

Moreover, not all fiber mixtures have synergizing effects with anthocyanins. FMA treatments did not present any synergistic effect. This difference is influenced by their structure and properties, which shape how well they can cooperate. For UC, this suggests that carefully selecting the right fibers can make the difference between average results and an effective formulation that improves butyrate production efficiency by reducing gas and improving tolerance in UC.

Recommendations

First, to develop and apply measuring methods compatible with fiber blends of variable pseudoplastic and precipitation nature. Measure solubility, viscosity, water-holding capacity, and any other relevant structural features that could influence fermentation rates. Viscosity measurements were attempted and were highly variable. These measurements will help define the differences between FMA and FMB in terms of fiber properties in relation to interaction with anthocyanins under UC conditions.

Second, to study and define the optimal range of viscosity, solubility, and fermentability that supports efficient fermentation in UC conditions. In this study, FMB was favored by its physicochemical characteristics. However, these outcomes can be further studied to find the optimal equilibrium and enhance fermentation efficiency. For each treatment, analyze total SCFA production, SCFA composition, butyrate production, and gas volume over time.

Finally, these findings should be complemented with *in vivo* testing of their anti-inflammatory properties and pathways for potentially reducing UC symptoms.

Referencias

Aliu, A., Bosch, D. H. C. A., Keszthelyi, D., Rezazadeh Ardabili, A., Colombel, J.-F [Jean-Frederic], Sawyer, R., Törnblom, H., Hart, A., Jonkers, D. M. A. E., Pierik, M. J. y Mujagic, Z. (2024). Review article: A practical approach to persistent gastrointestinal symptoms in inflammatory bowel disease in remission. *Alimentary Pharmacology & Therapeutics*, *59*(12), 1470–1488. https://doi.org/10.1111/apt.17988

Ananthakrishnan, A. N. (2015). Environmental risk factors for inflammatory bowel diseases: A review. *Digestive Diseases and Sciences*, *60*(2), 290–298. https://doi.org/10.1007/s10620-014-3350-9

Armstrong, H. K., Bording-Jorgensen, M., Santer, D. M., Zhang, Z., Valcheva, R., Rieger, A. M., Sung-Ho Kim, J., Dijk, S. I., Mahmood, R., Ogungbola, O., Jovel, J., Moreau, F., Gorman, H., Dickner, R., Jerasi, J., Mander, I. K., Lafleur, D., Cheng, C., Petrova, A., . . . Wine, E. (2023). Unfermented β-fructan Fibers Fuel Inflammation in Select Inflammatory Bowel Disease Patients. *Gastroenterology*, *164*(2), 228–240. https://doi.org/10.1053/j.gastro.2022.09.034

Arthur, J. C., Perez-Chanona, E., Mühlbauer, M., Tomkovich, S., Uronis, J. M., Fan, T.-J., Campbell, B. J., Abujamel, T., Dogan, B., Rogers, A. B., Rhodes, J. M., Stintzi, A., Simpson, K. W., Hansen, J. J., Keku, T. O., Fodor, A. A. y Jobin, C. (2012). Intestinal inflammation targets cancer-inducing activity of the microbiota. *Science (New York, N.Y.)*, *338*(6103), 120–123. https://doi.org/10.1126/science.1224820

Azad, M. A. K., Sarker, M., Li, T. y Yin, J. (2018). Probiotic Species in the Modulation of Gut Microbiota: An Overview. *BioMed Research International*, *2018*, 9478630. https://doi.org/10.1155/2018/9478630

Bai, A. H. C., Wu, W. K. K., Xu, L., Wong, S. H., Go, M. Y., Chan, A. W. H., Harbord, M., Zhang, S [Shenghong], Chen, M., Wu, J. C. Y., Chan, M. W. Y., Chan, M. T. V., Chan, F. K. L., Sung, J. J. Y., Yu, J., Cheng, A. S. L. y Ng, S. C. (2016). Dysregulated Lysine Acetyltransferase 2B Promotes Inflammatory Bowel Disease Pathogenesis Through Transcriptional Repression of Interleukin-10. *Journal of Crohn's & Colitis*, *10*(6), 726–734. https://doi.org/10.1093/ecco-jcc/jjw020

Bai, Y., Zhou, X., Zhao, J [Jinbiao], Wang, Z., Ye, H., Pi, Y., Che, D., Han, D., Zhang, S [Shuai] y Wang, J [Junjun] (2021). Sources of Dietary Fiber Affect the SCFA Production and Absorption in the Hindgut of Growing Pigs. *Frontiers in Nutrition*, *8*, 719935. https://doi.org/10.3389/fnut.2021.719935

Baldelli, V., Scaldaferri, F., Putignani, L. y Del Chierico, F. (2021). The Role of Enterobacteriaceae in Gut Microbiota Dysbiosis in Inflammatory Bowel Diseases. *Microorganisms*, *9*(4). https://doi.org/10.3390/microorganisms9040697

Bretin, A., Zou, J., San Yeoh, B., Ngo, V. L., Winer, S., Winer, D. A., Reddivari, L., Pellizzon, M., Walters, W. A., Patterson, A. D., Ley, R., Chassaing, B., Vijay-Kumar, M. y Gewirtz, A. T. (2023). Psyllium Fiber Protects Against Colitis Via Activation of Bile Acid Sensor Farnesoid X Receptor.

Cellular and Molecular Gastroenterology and Hepatology, *15*(6), 1421–1442. https://doi.org/10.1016/j.jcmgh.2023.02.007

Brodkorb, A., Egger, L., Alminger, M., Alvito, P., Assunção, R., Ballance, S., Bohn, T., Bourlieu-Lacanal, C., Boutrou, R., Carrière, F., Clemente, A., Corredig, M., Dupont, D., Dufour, C., Edwards, C., Golding, M., Karakaya, S., Kirkhus, B., Le Feunteun, S., . . . Recio, I. (2019). Infogest static in vitro simulation of gastrointestinal food digestion. *Nature Protocols*, *14*(4), 991–1014. https://doi.org/10.1038/s41596-018-0119-1

Bruscoli, S., Febo, M., Riccardi, C. y Migliorati, G. (2021). Glucocorticoid Therapy in Inflammatory Bowel Disease: Mechanisms and Clinical Practice. *Frontiers in Immunology*, *12*, 691480. https://doi.org/10.3389/fimmu.2021.691480

Bui, T. P. N., Troise, A. D., Fogliano, V. y Vos, W. M. de (2019). Anaerobic Degradation of N-ε-Carboxymethyllysine, a Major Glycation End-Product, by Human Intestinal Bacteria. *Journal of Agricultural and Food Chemistry*, *67*(23), 6594–6602. https://doi.org/10.1021/acs.jafc.9b02208

Byndloss, M. X., Olsan, E. E., Rivera-Chávez, F., Tiffany, C. R., Cevallos, S. A., Lokken, K. L., Torres, T. P., Byndloss, A. J., Faber, F., Gao, Y., Litvak, Y., Lopez, C. A., Xu, G., Napoli, E., Giulivi, C., Tsolis, R. M., Revzin, A., Lebrilla, C. B. y Bäumler, A. J. (2017). Microbiota-activated PPAR-γ signaling inhibits dysbiotic Enterobacteriaceae expansion. *Science (New York, N.Y.)*, *357*(6351), 570–575. https://doi.org/10.1126/science.aam9949

Campbell, A., Gdanetz, K., Schmidt, A. W. y Schmidt, T. M. (2023). H2 generated by fermentation in the human gut microbiome influences metabolism and competitive fitness of gut butyrate producers. *Microbiome*, *11*(1), 133. https://doi.org/10.1186/s40168-023-01565-3

Canfora, E. E., Meex, R. C. R., Venema, K. y Blaak, E. E. (2019). Gut microbial metabolites in obesity, NAFLD and T2DM. *Nature Reviews. Endocrinology*, *15*(5), 261–273. https://doi.org/10.1038/s41574-019-0156-z

Cantu-Jungles, T. M [T. M.], Agamennone, V., van den Broek, T. J., Schuren, F. H. J. y Hamaker, B [B.] (2025). Systematically-designed mixtures outperform single fibers for gut microbiota support. *Gut Microbes*, *17*(1), 2442521. https://doi.org/10.1080/19490976.2024.2442521

Cantu-Jungles, T. M [Thaisa M.], Bulut, N., Chambry, E., Ruthes, A., Iacomini, M., Keshavarzian, A., Johnson, T. A. y Hamaker, B. R. (2021). Dietary Fiber Hierarchical Specificity: The Missing Link for Predictable and Strong Shifts in Gut Bacterial Communities. *MBio*, *12*(3), e0102821. https://doi.org/10.1128/mbio.01028-21

Cantu-Jungles, T. M [Thaisa M.] y Hamaker, B. R. (2023). Tuning Expectations to Reality: Don't Expect Increased Gut Microbiota Diversity with Dietary Fiber. *The Journal of Nutrition*, *153*(11), 3156–3163. https://doi.org/10.1016/j.tjnut.2023.09.001

Cantu-Jungles, T. M [Thaisa M.], Rasmussen, H. E. y Hamaker, B. R. (2019). Potential of Prebiotic Butyrogenic Fibers in Parkinson's Disease. *Frontiers in Neurology*, *10*, 663. https://doi.org/10.3389/fneur.2019.00663

Cheng, B., Feng, H., Li, C [Cheng], Jia, F. y Zhang, X [Xiaowei] (2025). The mutual effect of dietary fiber and polyphenol on gut microbiota: Implications for the metabolic and microbial modulation and associated health benefits. *Carbohydrate Polymers*, *358*, 123541. https://doi.org/10.1016/j.carbpol.2025.123541

Cosier, D., Lambert, K., Batterham, M., Sanderson-Smith, M., Mansfield, K. J. y Charlton, K. (2024). The INHABIT (synergIstic effect of aNtHocyAnin and proBIoTics in) Inflammatory Bowel Disease trial: A study protocol for a double-blind, randomised, controlled, multi-arm trial. *Journal of Nutritional Science*, *13*, e1. https://doi.org/10.1017/jns.2023.113

Cross, R. K. (2017). Safety Considerations with the Use of Corticosteroids and Biologic Therapies in Mild-to-Moderate Ulcerative Colitis. *Inflammatory Bowel Diseases*, *23*(10), 1689–1701. https://doi.org/10.1097/mib.0000000000001261

Deehan, E. C., Duar, R. M., Armet, A. M., Perez-Muñoz, M. E., Jin, M. y Walter, J. (2017). Modulation of the Gastrointestinal Microbiome with Nondigestible Fermentable Carbohydrates To Improve Human Health. *Microbiology Spectrum*, *5*(5). https://doi.org/10.1128/microbiolspec.bad-0019-2017

Dell'Olio, A., Scott, W. T., Taroncher-Ferrer, S., San Onofre, N., Soriano, J. M. y Rubert, J. (2024). Tailored impact of dietary fibers on gut microbiota: A multi-omics comparison on the lean and obese microbial communities. *Microbiome*, *12*(1), 250. https://doi.org/10.1186/s40168-024-01975-x

Demidenko, E. y Miller, T. W. (2019). Statistical determination of synergy based on Bliss definition of drugs independence. *PloS One*, *14*(11), e0224137. https://doi.org/10.1371/journal.pone.0224137

Di Vincenzo, F., Del Gaudio, A., Petito, V., Lopetuso, L. R. y Scaldaferri, F. (2024). Gut microbiota, intestinal permeability, and systemic inflammation: A narrative review. *Internal and Emergency Medicine*, *19*(2), 275–293. https://doi.org/10.1007/s11739-023-03374-w

Dikeman, C. L. y Fahey, G. C. (2006). Viscosity as related to dietary fiber: A review. *Critical Reviews in Food Science and Nutrition*, *46*(8), 649–663. https://doi.org/10.1080/10408390500511862

Do, K.-H., Ko, S.-H., Kim, K. B., Seo, K. y Lee, W.-K. (2023). Comparative Study of Intestinal Microbiome in Patients with Ulcerative Colitis and Healthy Controls in Korea. *Microorganisms*, *11*(11). https://doi.org/10.3390/microorganisms11112750

Döring, C. y Basen, M. (2024). Propionate production by Bacteroidia gut bacteria and its dependence on substrate concentrations differs among species. *Biotechnology for Biofuels and Bioproducts*, *17*(1), 95. https://doi.org/10.1186/s13068-024-02539-9

Eckrote, S. y Reddivari, L. (2025). Anthocyanin and Pectin Complexes Attenuate Ulcerative Colitis in IL-10 Knockout Mice. *Inflammatory Bowel Diseases*, *31*(Supplement_1), S3-S3. https://doi.org/10.1093/ibd/izae282.006

Facchin, S., Bertin, L., Bonazzi, E., Lorenzon, G., Barba, C. de, Barberio, B., Zingone, F., Maniero, D., Scarpa, M., Ruffolo, C., Angriman, I. y Savarino, E. V. (2024). Short-Chain Fatty Acids and Human Health: From Metabolic Pathways to Current Therapeutic Implications. *Life (Basel, Switzerland)*, *14*(5). https://doi.org/10.3390/life14050559

Feng, W., Liu, J [Juan], Cheng, H., Zhang, D [Dandan], Tan, Y. y Peng, C. (2022). Dietary compounds in modulation of gut microbiota-derived metabolites. *Frontiers in Nutrition*, *9*, 939571. https://doi.org/10.3389/fnut.2022.939571

Fernandes, A., Mateus, N. y Freitas, V. de (2023). Polyphenol-Dietary Fiber Conjugates from Fruits and Vegetables: Nature and Biological Fate in a Food and Nutrition Perspective. *Foods (Basel, Switzerland)*, *12*(5). https://doi.org/10.3390/foods12051052

Fernández-Veledo, S., Grau-Bové, C., Notararigo, S. y Huber-Ruano, I. (2025). The role of microbial succinate in the pathophysiology of inflammatory bowel disease: Mechanisms and therapeutic potential. *Current Opinion in Microbiology*, *85*, 102599. https://doi.org/10.1016/j.mib.2025.102599

Foucquier, J. y Guedj, M. (2015). Analysis of drug combinations: Current methodological landscape. *Pharmacology Research & Perspectives*, *3*(3), e00149. https://doi.org/10.1002/prp2.149

Fu, W., Li, S [Shiyu], Helmick, H., Hamaker, B. R., Kokini, J. L. y Reddivari, L. (2023). Complexation with Polysaccharides Enhances the Stability of Isolated Anthocyanins. *Foods (Basel, Switzerland)*, *12*(9). https://doi.org/10.3390/foods12091846

Fukuda, T., Naganuma, M. y Kanai, T. (2019). Current new challenges in the management of ulcerative colitis. *Intestinal Research*, *17*(1), 36–44. https://doi.org/10.5217/ir.2018.00126

Gillis, C. C., Hughes, E. R., Spiga, L., Winter, M. G., Zhu, W [Wenhan], Furtado de Carvalho, T., Chanin, R. B., Behrendt, C. L., Hooper, L. V., Santos, R. L. y Winter, S. E. (2018). Dysbiosis-Associated Change in Host Metabolism Generates Lactate to Support Salmonella Growth. *Cell Host & Microbe*, *23*(1), 54-64.e6. https://doi.org/10.1016/j.chom.2017.11.006

GraphPad Software. (2024)). *Statistics guide: Bliss independence and drug synergy.* https://www.graphpad.com/guides/prism/latest/statistics/index.htm

Greco, W. R., Bravo, G. y Parsons, J. C. (1995). The search for synergy: A critical review from a response surface perspective. *Pharmacological Reviews*, *47*(2), 331–385.

Gunn, D., Abbas, Z., Harris, H. C., Major, G., Hoad, C., Gowland, P., Marciani, L., Gill, S. K., Warren, F. J [Fred J.], Rossi, M., Remes-Troche, J. M., Whelan, K. y Spiller, R. C. (2022). Psyllium reduces

inulin-induced colonic gas production in IBS: Mri and in vitro fermentation studies. *Gut*, *71*(5), 919–927. https://doi.org/10.1136/gutjnl-2021-324784

Hamaker, B. R. y Cantu-Jungles, T. M [Thaisa Moro] (2020). Discrete Fiber Structures Dictate Human Gut Bacteria Outcomes. *Trends in Endocrinology and Metabolism: TEM*, *31*(11), 803–805. https://doi.org/10.1016/j.tem.2020.05.002

Hamaker, B. R. y Tuncil, Y. E. (2014). A perspective on the complexity of dietary fiber structures and their potential effect on the gut microbiota. *Journal of Molecular Biology*, *426*(23), 3838–3850. https://doi.org/10.1016/j.jmb.2014.07.028

Harris, H. C., Pereira, N., Koev, T., Khimyak, Y. Z., Yakubov, G. E. y Warren, F. J [Frederick J.] (2023). The impact of psyllium gelation behaviour on in vitro colonic fermentation properties. *Food Hydrocolloids*, *139*, 108543. https://doi.org/10.1016/j.foodhyd.2023.108543

He, X., Sun, C., Zhao, J [Jingwen], Zhang, Y [Yin], Zhang, X [Xiaowei] y Fang, Y. (2023). High Viscosity Slows the Utilization of Rapidly Fermentable Dietary Fiber by Human Gut Microbiota. *Journal of Agricultural and Food Chemistry*, *71*(48), 19078–19087. https://doi.org/10.1021/acs.jafc.3c05652

Heinzel, S., Jureczek, J., Kainulainen, V., Nieminen, A. I., Suenkel, U., Thaler, A.-K. von, Kaleta, C., Eschweiler, G. W., Brockmann, K., Aho, V. T. E., Auvinen, P., Maetzler, W., Berg, D. y Scheperjans, F. (2024). Elevated fecal calprotectin is associated with gut microbial dysbiosis, altered serum markers and clinical outcomes in older individuals. *Scientific Reports*, *14*(1), 13513. https://doi.org/10.1038/s41598-024-63893-0

Hou, K., Wu, Z.-X., Chen, X.-Y., Wang, J.-Q., Zhang, D [Dongya], Xiao, C., Zhu, D., Koya, J. B., Wei, L., Li, J [Jilin] y Chen, Z.-S. (2022). Microbiota in health and diseases. *Signal Transduction and Targeted Therapy*, *7*(1), 135. https://doi.org/10.1038/s41392-022-00974-4

Huo, L., Chen, Q., Jia, S., Zhang, Y [Yuli], Wang, L., Li, X [Xian], Li, Z., Sun, B., Shan, J., Lin, J., Yang, L. y Sui, H. (2025). Gut microbiome promotes succinate-induced ulcerative colitis by enhancing glycolysis through SUCNR1/NF-κB signaling pathway. *American Journal of Physiology. Cell Physiology*, *329*(2), C440-C454. https://doi.org/10.1152/ajpcell.00411.2025

Jakobek, L., Strelec, I., Kenjerić, D., Šoher, L., Tomac, I. y Matić, P. (2022). Simulated Gastric and Intestinal Fluid Electrolyte Solutions as an Environment for the Adsorption of Apple Polyphenols onto β-Glucan. *Molecules (Basel, Switzerland)*, *27*(19). https://doi.org/10.3390/molecules27196683

Jalanka, J., Major, G., Murray, K., Singh, G., Nowak, A., Kurtz, C., Silos-Santiago, I., Johnston, J. M., Vos, W. M. de y Spiller, R. (2019). The Effect of Psyllium Husk on Intestinal Microbiota in Constipated Patients and Healthy Controls. *International Journal of Molecular Sciences*, *20*(2). https://doi.org/10.3390/ijms20020433

Jangi, S., Zhao, N., Hsia, K., Park, Y. S., Michaud, D. S. y Yoon, H. (2025). Specific Bacterial Co-abundance Groups Are Associated With Inflammatory Status in Patients With Ulcerative Colitis. *Journal of Crohn's & Colitis*, *19*(1). https://doi.org/10.1093/ecco-jcc/jjae125

Kabisch, S., Hajir, J., Sukhobaevskaia, V., Weickert, M. O. y Pfeiffer, A. F. H. (2025). Impact of Dietary Fiber on Inflammation in Humans. *International Journal of Molecular Sciences*, *26*(5). https://doi.org/10.3390/ijms26052000

Kapoor, P., Tiwari, A., Sharma, S., Tiwari, V., Sheoran, B., Ali, U. y Garg, M. (2023). Effect of anthocyanins on gut health markers, Firmicutes-Bacteroidetes ratio and short-chain fatty acids: A systematic review via meta-analysis. *Scientific Reports*, *13*(1), 1729. https://doi.org/10.1038/s41598-023-28764-0

Kappelman, M. D., Brensinger, C., Parlett, L. E., Hurtado-Lorenzo, A. y Lewis, J. D. (2025). Prevalence of Pediatric Inflammatory Bowel Disease in the United States: Pooled Estimates From Three Administrative Claims Data Sources. *Gastroenterology*, *168*(5), 980-982.e2. https://doi.org/10.1053/j.gastro.2024.11.004

Khoo, H. E., Azlan, A., Tang, S. T. y Lim, S. M. (2017). Anthocyanidins and anthocyanins: Colored pigments as food, pharmaceutical ingredients, and the potential health benefits. *Food & Nutrition Research*, *61*(1), 1361779. https://doi.org/10.1080/16546628.2017.1361779

Kobayashi, T., Siegmund, B., Le Berre, C., Wei, S. C., Ferrante, M., Shen, B., Bernstein, C. N., Danese, S., Peyrin-Biroulet, L. y Hibi, T. (2020). Ulcerative colitis. *Nature Reviews. Disease Primers*, *6*(1), 74. https://doi.org/10.1038/s41572-020-0205-x

Koh, J., Xu, Z [Zhimin] y Wicker, L. (2020). Blueberry pectin and increased anthocyanins stability under in vitro digestion. *Food Chemistry*, *302*, 125343. https://doi.org/10.1016/j.foodchem.2019.125343

Kumar, N. y Goel, N. (2019). Phenolic acids: Natural versatile molecules with promising therapeutic applications. *Biotechnology Reports (Amsterdam, Netherlands)*, *24*, e00370. https://doi.org/10.1016/j.btre.2019.e00370

Lachmansingh, D. A., Valderrama, B., Bastiaanssen, T., Cryan, J., Clarke, G. y Lavelle, A. (2023). Impact of dietary fiber on gut microbiota composition, function and gut-brain-modules in healthy adults - a systematic review protocol. *HRB Open Research*, *6*, 62. https://doi.org/10.12688/hrbopenres.13794.2

Lante, A., Canazza, E. y Tessari, P. (2023). Beta-Glucans of Cereals: Functional and Technological Properties. *Nutrients*, *15*(9). https://doi.org/10.3390/nu15092124

Larsen, L. R., Buerschaper, J., Schieber, A. y Weber, F. (2019). Interactions of Anthocyanins with Pectin and Pectin Fragments in Model Solutions. *Journal of Agricultural and Food Chemistry*, *67*(33), 9344–9353. https://doi.org/10.1021/acs.jafc.9b03108

Lee, J.-Y., Tsolis, R. M. y Bäumler, A. J. (2022). The microbiome and gut homeostasis. *Science (New York, N.Y.)*, *377*(6601), eabp9960. https://doi.org/10.1126/science.abp9960

Li, D., Liu, Z., Fan, X., Zhao, T., Wen, D., Huang, X. y Li, B. (2024). Lactic Acid Bacteria-Gut-Microbiota-Mediated Intervention towards Inflammatory Bowel Disease. *Microorganisms*, *12*(9). https://doi.org/10.3390/microorganisms12091864

Li, H., Christman, L. M., Li, R. y Gu, L. (2020). Synergic interactions between polyphenols and gut microbiota in mitigating inflammatory bowel diseases. *Food & Function*, *11*(6), 4878–4891. https://doi.org/10.1039/d0fo00713g

Li, L.-L., Wang, Y.-T., Zhu, L.-M., Liu, Z.-Y., Ye, C.-Q. y Qin, S. (2020). Inulin with different degrees of polymerization protects against diet-induced endotoxemia and inflammation in association with gut microbiota regulation in mice. *Scientific Reports*, *10*(1), 978. https://doi.org/10.1038/s41598-020-58048-w

Litvak, Y., Byndloss, M. X. y Bäumler, A. J. (2018). Colonocyte metabolism shapes the gut microbiota. *Science (New York, N.Y.)*, *362*(6418). https://doi.org/10.1126/science.aat9076

Lopez-Siles, M., Enrich-Capó, N., Aldeguer, X., Sabat-Mir, M., Duncan, S. H., Garcia-Gil, L. J. y Martinez-Medina, M. (2018). Alterations in the Abundance and Co-occurrence of Akkermansia muciniphila and Faecalibacterium prausnitzii in the Colonic Mucosa of Inflammatory Bowel Disease Subjects. *Frontiers in Cellular and Infection Microbiology*, *8*, 281. https://doi.org/10.3389/fcimb.2018.00281

Louis, P. y Flint, H. J. (2017). Formation of propionate and butyrate by the human colonic microbiota. *Environmental Microbiology*, *19*(1), 29–41. https://doi.org/10.1111/1462-2920.13589

Louis, P., Solvang, M., Duncan, S. H., Walker, A. W. y Mukhopadhya, I. (2021). Dietary fibre complexity and its influence on functional groups of the human gut microbiota. *Proceedings of the Nutrition Society*, *80*(4), 386–397. https://doi.org/10.1017/S0029665121003694

Lozupone, C. A., Stombaugh, J. I., Gordon, J. I., Jansson, J. K. y Knight, R. (2012). Diversity, stability and resilience of the human gut microbiota. *Nature*, *489*(7415), 220–230. https://doi.org/10.1038/nature11550

Ma, N., Tian, Y., Wu, Y [Yi] y Ma, X. (2017). Contributions of the Interaction Between Dietary Protein and Gut Microbiota to Intestinal Health. *Current Protein & Peptide Science*, *18*(8), 795–808. https://doi.org/10.2174/1389203718666170216153505

Machiels, K., Joossens, M., Sabino, J., Preter, V. de, Arijs, I., Eeckhaut, V., Ballet, V., Claes, K., van Immerseel, F., Verbeke, K., Ferrante, M., Verhaegen, J., Rutgeerts, P. y Vermeire, S. (2014). A decrease of the butyrate-producing species Roseburia hominis and Faecalibacterium prausnitzii defines dysbiosis in patients with ulcerative colitis. *Gut*, *63*(8), 1275–1283. https://doi.org/10.1136/gutjnl-2013-304833

Maiuolo, J., Bulotta, R. M., Ruga, S., Nucera, S., Macrì, R., Scarano, F., Oppedisano, F., Carresi, C., Gliozzi, M., Musolino, V., Mollace, R., Muscoli, C. y Mollace, V. (2024). The Postbiotic Properties of Butyrate in the Modulation of the Gut Microbiota: The Potential of Its Combination with Polyphenols and Dietary Fibers. *International Journal of Molecular Sciences*, *25*(13). https://doi.org/10.3390/ijms25136971

Makki, K., Deehan, E. C., Walter, J. y Bäckhed, F. (2018). The Impact of Dietary Fiber on Gut Microbiota in Host Health and Disease. *Cell Host & Microbe*, *23*(6), 705–715. https://doi.org/10.1016/j.chom.2018.05.012

Milajerdi, A., Ebrahimi-Daryani, N., Dieleman, L. A., Larijani, B. y Esmaillzadeh, A. (2021). Association of Dietary Fiber, Fruit, and Vegetable Consumption with Risk of Inflammatory Bowel Disease: A Systematic Review and Meta-Analysis. *Advances in Nutrition (Bethesda, Md.)*, *12*(3), 735–743. https://doi.org/10.1093/advances/nmaa145

Mocanu, V. y Madsen, K. L. (2024). Dietary fibre and metabolic health: A clinical primer. *Clinical and Translational Medicine*, *14*(10), e70018. https://doi.org/10.1002/ctm2.70018

Moncada, E., Bulut, N., Li, S [Shiyu], Johnson, T., Hamaker, B. y Reddivari, L. (2024). Dietary Fiber's Physicochemical Properties and Gut Bacterial Dysbiosis Determine Fiber Metabolism in the Gut. *Nutrients*, *16*(15). https://doi.org/10.3390/nu16152446

Muro, P., Zhang, L [Li], Li, S [Shuxuan], Zhao, Z., Jin, T., Mao, F. y Mao, Z. (2024). The emerging role of oxidative stress in inflammatory bowel disease. *Frontiers in Endocrinology*, *15*, 1390351. https://doi.org/10.3389/fendo.2024.1390351

Mutaz, S. (2024). *Ulcerative Colitis in Children: Background, Epidemiology, Prognosis*. https://emedicine.medscape.com/article/930146-overview?form=fpf

Mutuyemungu, E., Singh, M., Liu, S. y Rose, D. J. (2023). Intestinal gas production by the gut microbiota: A review. *Journal of Functional Foods*, *100*, 105367. https://doi.org/10.1016/j.jff.2022.105367

Nagano, T., Higashimura, Y., Nakano, M., Nishiuchi, T. y Lelo, A. P. (2025). High-viscosity dietary fibers modulate gut microbiota and liver metabolism to prevent obesity in high-fat diet-fed mice. *International Journal of Biological Macromolecules*, *298*, 139962. https://doi.org/10.1016/j.ijbiomac.2025.139962

Nemzer, B. V., Al-Taher, F., Kalita, D., Yashin, A. Y. y Yashin, Y. I. (2025). Health-Improving Effects of Polyphenols on the Human Intestinal Microbiota: A Review. *International Journal of Molecular Sciences*, *26*(3). https://doi.org/10.3390/ijms26031335

Nishino, K., Nishida, A., Inoue, R., Kawada, Y., Ohno, M., Sakai, S., Inatomi, O., Bamba, S., Sugimoto, M., Kawahara, M., Naito, Y. y Andoh, A. (2018). Analysis of endoscopic brush samples identified mucosa-associated dysbiosis in inflammatory bowel disease. *Journal of Gastroenterology*, *53*(1), 95–106. https://doi.org/10.1007/s00535-017-1384-4

Noguer, M. C., Escudié, R., Bernet, N. y Eric, T. (2022). Populational and metabolic shifts induced by acetate, butyrate and lactate in dark fermentation. *International Journal of Hydrogen Energy*, *47*(66), 28385–28398. https://doi.org/10.1016/j.ijhydene.2022.06.163

Ozdal, T., Sela, D. A., Xiao, J., Boyacioglu, D., Chen, F. y Capanoglu, E. (2016). The Reciprocal Interactions between Polyphenols and Gut Microbiota and Effects on Bioaccessibility. *Nutrients*, *8*(2), 78. https://doi.org/10.3390/nu8020078

Parada Venegas, D., La Fuente, M. K. de, Landskron, G., González, M. J., Quera, R., Dijkstra, G., Harmsen, H. J. M., Faber, K. N. y Hermoso, M. A. (2019). Short Chain Fatty Acids (SCFAs)-Mediated Gut Epithelial and Immune Regulation and Its Relevance for Inflammatory Bowel Diseases. *Frontiers in Immunology*, *10*, 277. https://doi.org/10.3389/fimmu.2019.00277

Park, B., Kim, J. Y., Riffey, O. F., Walsh, T. J., Johnson, J. y Donohoe, D. R. (2024). Crosstalk between butyrate oxidation in colonocyte and butyrate-producing bacteria. *IScience*, *27*(9), 110853. https://doi.org/10.1016/j.isci.2024.110853

Pasinetti, G. M., Singh, R., Westfall, S., Herman, F., Faith, J. y Ho, L. (2018). The Role of the Gut Microbiota in the Metabolism of Polyphenols as Characterized by Gnotobiotic Mice. *Journal of Alzheimer's Disease : JAD*, *63*(2), 409–421. https://doi.org/10.3233/jad-171151

Pirkola, L., Dicksved, J., Loponen, J., Marklinder, I. y Andersson, R. (2023). Fecal microbiota composition affects in vitro fermentation of rye, oat, and wheat bread. *Scientific Reports*, *13*(1), 99. https://doi.org/10.1038/s41598-022-26847-y

Putignani, L., Oliva, S., Isoldi, S., Del Chierico, F., Carissimi, C., Laudadio, I., Cucchiara, S. y Stronati, L. (2021). Fecal and mucosal microbiota profiling in pediatric inflammatory bowel diseases. *European Journal of Gastroenterology & Hepatology*, *33*(11), 1376–1386. https://doi.org/10.1097/meg.0000000000002050

Quaglio, A. E. V., Grillo, T. G., Oliveira, E. C. S. de, Di Stasi, L. C. y Sassaki, L. Y. (2022). Gut microbiota, inflammatory bowel disease and colorectal cancer. *World Journal of Gastroenterology*, *28*(30), 4053–4060. https://doi.org/10.3748/wjg.v28.i30.4053

Quince, C., Walker, A. W., Simpson, J. T., Loman, N. J. y Segata, N. (2017). Shotgun metagenomics, from sampling to analysis. *Nature Biotechnology*, *35*(9), 833–844. https://doi.org/10.1038/nbt.3935

Raj, A., Rifkin, S. A., Andersen, E. y van Oudenaarden, A. (2010). Variability in gene expression underlies incomplete penetrance. *Nature*, *463*(7283), 913–918. https://doi.org/10.1038/nature08781

Ray, S. K. y Mukherjee, S. (2021). Evolving Interplay Between Dietary Polyphenols and Gut Microbiota-An Emerging Importance in Healthcare. *Frontiers in Nutrition*, *8*, 634944. https://doi.org/10.3389/fnut.2021.634944

Recharla, N., Geesala, R. y Shi, X.-Z. (2023). Gut Microbial Metabolite Butyrate and Its Therapeutic Role in Inflammatory Bowel Disease: A Literature Review. *Nutrients*, *15*(10). https://doi.org/10.3390/nu15102275

Requena, T., Martínez-Cuesta, M. C. y Peláez, C. (2018). Diet and microbiota linked in health and disease. *Food & Function*, *9*(2), 688–704. https://doi.org/10.1039/C7FO01820G

Rodríguez-Daza, M. C., Pulido-Mateos, E. C., Lupien-Meilleur, J., Guyonnet, D., Desjardins, Y. y Roy, D. (2021). Polyphenol-Mediated Gut Microbiota Modulation: Toward Prebiotics and Further. *Frontiers in Nutrition*, *8*, 689456. https://doi.org/10.3389/fnut.2021.689456

Schoelmerich, M. C. y Müller, V. (2020). Energy-converting hydrogenases: The link between H2 metabolism and energy conservation. *Cellular and Molecular Life Sciences : CMLS*, *77*(8), 1461–1481. https://doi.org/10.1007/s00018-019-03329-5

Sejbuk, M., Mirończuk-Chodakowska, I., Karav, S. y Witkowska, A. M. (2024). Dietary Polyphenols, Food Processing and Gut Microbiome: Recent Findings on Bioavailability, Bioactivity, and Gut Microbiome Interplay. *Antioxidants (Basel, Switzerland)*, *13*(10). https://doi.org/10.3390/antiox13101220

Sejbuk, M., Siebieszuk, A. y Witkowska, A. M. (2024). The Role of Gut Microbiome in Sleep Quality and Health: Dietary Strategies for Microbiota Support. *Nutrients*, *16*(14). https://doi.org/10.3390/nu16142259

Shi, C., Guo, C., Wang, S [Shan], Li, W., Zhang, X [Xue], Lu, S., Ning, C. y Tan, C. (2024). The mechanism of pectin in improving anthocyanin stability and the application progress of their complexes: A review. *Food Chemistry: X*, *24*, 101955. https://doi.org/10.1016/j.fochx.2024.101955

Singh, V., Lee, G., Son, H., Koh, H., Kim, E. S., Unno, T. y Shin, J.-H. (2022). Butyrate producers, "The Sentinel of Gut": Their intestinal significance with and beyond butyrate, and prospective use as microbial therapeutics. *Frontiers in Microbiology*, *13*, 1103836. https://doi.org/10.3389/fmicb.2022.1103836

Srinivasan, L. V. y Rana, S. S. (2025). Anthocyanins: a promising source of natural colorants and nutraceuticals. *Discover Applied Sciences*, *7*(7). https://doi.org/10.1007/s42452-025-07196-7

Staudacher, H. M., Irving, P. M., Lomer, M. C. E. y Whelan, K. (2014). Mechanisms and efficacy of dietary FODMAP restriction in IBS. *Nature Reviews. Gastroenterology & Hepatology*, *11*(4), 256–266. https://doi.org/10.1038/nrgastro.2013.259

Steinsbø, Ø., Carlsen, A., Aasprong, O. G., Aabakken, L., Tvedt-Gundersen, E., Bjørkhaug, S., Gjerde, R., Normann Karlsen, L. y Grimstad, T. (2022). Histologic healing and factors associated with complete remission following conventional treatment in ulcerative colitis. *Therapeutic Advances in Gastroenterology*, *15*, 17562848221140659. https://doi.org/10.1177/17562848221140659

Stummer, N., Feichtinger, R. G., Weghuber, D., Kofler, B. y Schneider, A. M. (2023). Role of Hydrogen Sulfide in Inflammatory Bowel Disease. *Antioxidants (Basel, Switzerland)*, *12*(8). https://doi.org/10.3390/antiox12081570

Sugihara, K. y Kamada, N. (2021). Diet-Microbiota Interactions in Inflammatory Bowel Disease. *Nutrients*, *13*(5). https://doi.org/10.3390/nu13051533

Takahashi, K., Nishida, A., Fujimoto, T., Fujii, M., Shioya, M., Imaeda, H., Inatomi, O., Bamba, S., Sugimoto, M. y Andoh, A. (2016). Reduced Abundance of Butyrate-Producing Bacteria Species in the Fecal Microbial Community in Crohn's Disease. *Digestion*, *93*(1), 59–65. https://doi.org/10.1159/000441768

Tang, R., He, Y. y Fan, K. (2023). Recent advances in stability improvement of anthocyanins by efficient methods and its application in food intelligent packaging: A review. *Food Bioscience*, *56*, 103164. https://doi.org/10.1016/j.fbio.2023.103164

Thilavech, T., Suantawee, T., Chusak, C., Suklaew, P. O. y Adisakwattana, S. (2025). Black rice (Oryza sativa L.) and its anthocyanins: mechanisms, food applications, and clinical insights for postprandial glycemic and lipid regulation. *Food Production, Processing and Nutrition*, *7*(1). https://doi.org/10.1186/s43014-024-00288-8

Tuncil, Y. E., Thakkar, R. D., Marcia, A. D. R., Hamaker, B. R. y Lindemann, S. R. (2018). Divergent short-chain fatty acid production and succession of colonic microbiota arise in fermentation of variously-sized wheat bran fractions. *Scientific Reports*, *8*(1), 16655. https://doi.org/10.1038/s41598-018-34912-8

Ungaro, R., Mehandru, S., Allen, P. B., Peyrin-Biroulet, L. y Colombel, J.-F [Jean-Frédéric] (2017). Ulcerative colitis. *Lancet (London, England)*, *389*(10080), 1756–1770. https://doi.org/10.1016/s0140-6736(16)32126-2

Valles-Colomer, M., Falony, G., Darzi, Y., Tigchelaar, E. F., Wang, J [Jun], Tito, R. Y., Schiweck, C., Kurilshikov, A., Joossens, M., Wijmenga, C., Claes, S., van Oudenhove, L., Zhernakova, A., Vieira-Silva, S. y Raes, J. (2019). The neuroactive potential of the human gut microbiota in quality of life and depression. *Nature Microbiology*, *4*(4), 623–632. https://doi.org/10.1038/s41564-018-0337-x

Van-Wehle, T. y Vital, M. (2024). Investigating the response of the butyrate production potential to major fibers in dietary intervention studies. *NPJ Biofilms and Microbiomes*, *10*(1), 63. https://doi.org/10.1038/s41522-024-00533-5

Verediano, T. A., Stampini Duarte Martino, H., Dias Paes, M. C. y Tako, E. (2021). Effects of Anthocyanin on Intestinal Health: A Systematic Review. *Nutrients*, *13*(4). https://doi.org/10.3390/nu13041331

Wang, S [Shaokang], Zhang, B., Chen, T., Li, C [Chao], Fu, X. y Huang, Q. (2019). Chemical Cross-Linking Controls in Vitro Fecal Fermentation Rate of High-Amylose Maize Starches and Regulates Gut

Microbiota Composition. *Journal of Agricultural and Food Chemistry*, *67*(49), 13728–13736. https://doi.org/10.1021/acs.jafc.9b04410

Williams, B. A., Mikkelsen, D., Flanagan, B. M. y Gidley, M. J. (2019). "Dietary fibre": Moving beyond the "soluble/insoluble" classification for monogastric nutrition, with an emphasis on humans and pigs. *Journal of Animal Science and Biotechnology*, *10*, 45. https://doi.org/10.1186/s40104-019-0350-9

Winter, S. E. y Bäumler, A. J. (2014). Dysbiosis in the inflamed intestine: Chance favors the prepared microbe. *Gut Microbes*, *5*(1), 71–73. https://doi.org/10.4161/gmic.27129

Xu, J., Xu, R., Jia, M., Su, Y. y Zhu, W [Weiyun] (2021). Metatranscriptomic analysis of colonic microbiota's functional response to different dietary fibers in growing pigs. *Animal Microbiome*, *3*(1), 45. https://doi.org/10.1186/s42523-021-00108-1

Yang, Z., Huang, T., Li, P., Ai, J., Liu, J [Jiaxin], Bai, W. y Tian, L. (2021). Dietary Fiber Modulates the Fermentation Patterns of Cyanidin-3-O-Glucoside in a Fiber-Type Dependent Manner. *Foods (Basel, Switzerland)*, *10*(6). https://doi.org/10.3390/foods10061386

Yarur, A. J., Strobel, S. G., Deshpande, A. R. y Abreu, M. T. (2011). Predictors of aggressive inflammatory bowel disease. *Gastroenterology & Hepatology*, *7*(10), 652–659.

Zhang, D [Dan], Jian, Y.-P., Zhang, Y.-N., Li, Y., Gu, L.-T., Sun, H.-H., Liu, M.-D., Zhou, H.-L., Wang, Y.-S. y Xu, Z.-X. (2023). Short-chain fatty acids in diseases. *Cell Communication and Signaling : CCS*, *21*(1), 212. https://doi.org/10.1186/s12964-023-01219-9

Zhang, M., Sun, K., Wu, Y [Yujun], Yang, Y., Tso, P. y Wu, Z. (2017). Interactions between Intestinal Microbiota and Host Immune Response in Inflammatory Bowel Disease. *Frontiers in Immunology*, *8*, 942. https://doi.org/10.3389/fimmu.2017.00942

Zhang, Y [Yi], Xu, Z [Zhiqiang], Gu, Z., Cheng, L., Hong, Y. y Li, L. (2025). Effect of anthocyanins on the in vitro fermentation of high-amylose starch. *Carbohydrate Polymers*, *353*, 123271. https://doi.org/10.1016/j.carbpol.2025.123271

Zhao, W., Sachsenmeier, K., Zhang, L [Lanju], Sult, E., Hollingsworth, R. E. y Yang, H. (2014). A New Bliss Independence Model to Analyze Drug Combination Data. *Journal of Biomolecular Screening*, *19*(5), 817–821. https://doi.org/10.1177/1087057114521867

Zhu, L., Guo, F., Guo, Z., Chen, X., Qian, X., Li, X [Xianglong], Li, X [Xiaoqiong], Li, J [Jinjun], Wang, X. y Jia, W. (2022). Potential health benefits of lowering gas production and bifidogenic effect of the blends of polydextrose with inulin in a human gut model. *Frontiers in Nutrition*, *9*, 934621. https://doi.org/10.3389/fnut.2022.934621

Ziętek, M., Celewicz, Z. y Szczuko, M. (2021). Short-Chain Fatty Acids, Maternal Microbiota and Metabolism in Pregnancy. *Nutrients*, *13*(4). https://doi.org/10.3390/nu13041244

Appendices

Appendix A

Shannon Entropy 24-Hour Timepoint

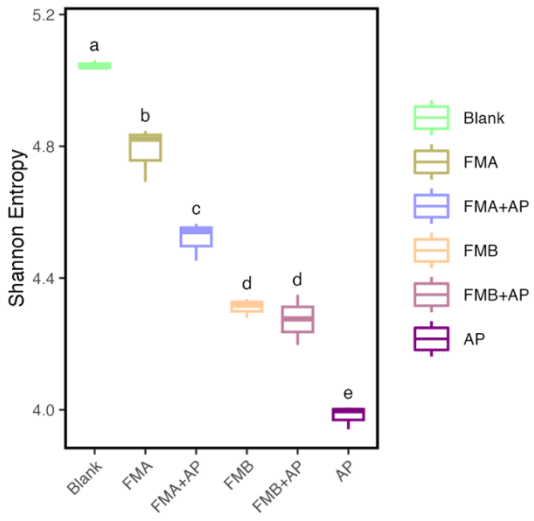

Appendix B

Shannon Entropy 48-hour timepoint

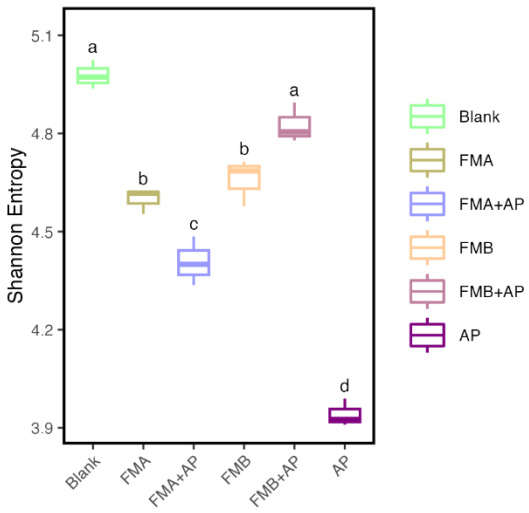

Appendix C

Genus relative Abundance at 24 and 48 hours

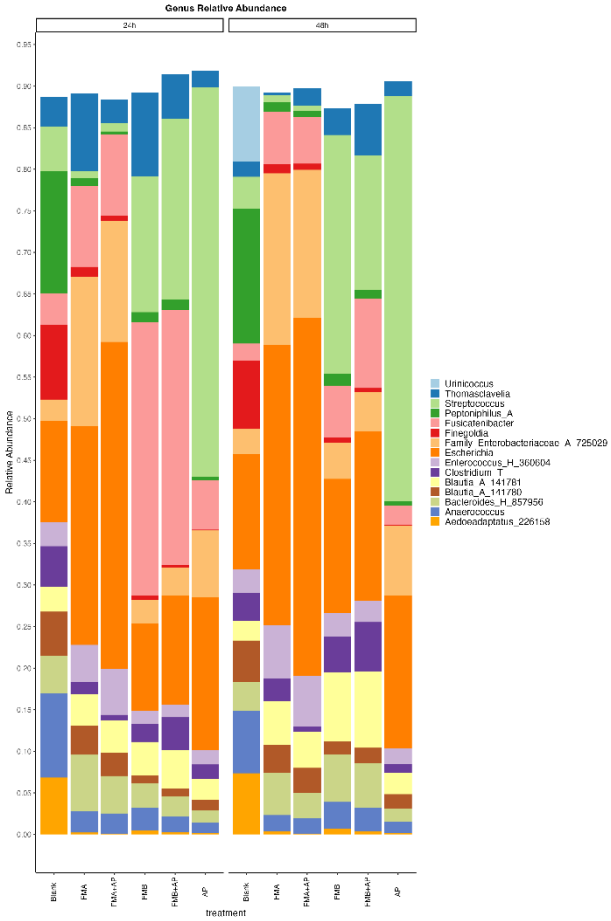

Appendix D

Statistical analysis for SCFA Composition (%) 48 hours

SCFA (%)	Blank	FMA	FMA+AP	FMB	FMB+AP	AP
Acetate (%)	70.2±1.06^{b}	77.4±0.38^{a}	77.5±1.18^{a}	69.1±0.11^{b}	68.5±0.11^{b}	62.7±1.82^{c}
Propionate (%)	13.5±0.45^{c}	10.3±0.08^{d}	11.9±0.29^{cd}	18.3±0.52^{b}	17.1±0.91^{b}	30.9±1.85^{a}
Butyrate (%)	15.7±0.66^{a}	12.1±0.30^{b}	10.5±0.90^{c}	12.5±0.47^{b}	14.0±0.87^{a}	6.2±0.16^{d}

Appendix E

Statistical analysis for SCFA Composition (%) 12 hours

SCFA (%)	Blank	FMA	FMA+AP	FMB	FMB+AP	AP
Acetate (%)	77.9 ± 3.27^{c}	87.8 ± 1.07^{ab}	90.2 ± 0.03^{a}	84.9 ± 0.51^{b}	85.0 ± 1.8^{b}	84.6 ± 0.32^{b}
Propionate (%)	10.2 ± 1.31^{a}	4.8 ± 0.41^{bc}	4.5 ± 0.05^{c}	5.4 ± 0.18^{bc}	6.2 ± 0.58^{b}	9.2 ± 0.21^{a}
Butyrate (%)	11.8 ± 1.96^{a}	7.3 ± 0.66^{bc}	5.1 ± 0.06^{d}	9.5 ± 0.44^{ab}	8.6 ± 1.22^{bc}	6.1 ± 0.26^{cd}